Benchmark Control Problems for Seismically Excited Nonlinear Buildings

Y. Ohtori[1], R.E. Christenson and B.F. Spencer, Jr.
Department of Civil Engineering and Geological Sciences
University of Notre Dame, Notre Dame, Indiana 46556-0767, USA

and

S.J. Dyke
Department of Civil Engineering
Washington University, St. Louis, Missouri 63130, USA

Abstract

This paper presents the problem definition and guidelines of a set of benchmark control problems for seismically excited nonlinear buildings. Focusing on three typical steel structures, 3-, 9- and 20-story buildings designed for the SAC project for the Los Angeles, California region, the goal of this study is to provide a clear basis to evaluate the efficacy of various structural control strategies. A nonlinear evaluation model has been developed that portrays the salient features of the structural system. Evaluation criteria and control constraints are presented for the design problems. The task of each participant in this benchmark study is to define (including sensors and control algorithms), evaluate and report on their proposed control strategies. These strategies may be either passive, active, semi-active or a combination thereof. The benchmark control problems will then facilitate direct comparison of the relative merits of the various control strategies. To illustrate some of the design challenges, a sample control strategy employing active control with a linear quadratic Gaussian (LQG) control algorithm is applied to the 20-story structure.

Introduction

The protection of civil structures, including material content and human occupants, is, without doubt, a world-wide priority. The extent of protection may range from reliable operation and occupant comfort to human and structural survivability. Civil structures, including existing and future buildings, towers and bridges, must be adequately protected from a variety of events, including earthquakes, winds, waves and traffic. The protection of structures is now moving from reliance entirely on the inelastic deformation of the structure to dissipate the energy of severe dynamic loadings, to the application of passive, active and semi-active structural control devices to mitigate undesired responses to dynamic loads. However, even in controlled structures, it can be expected that large seismic events, such as the 1994 Northridge and the 1995 Kobe earthquakes, will cause structural members to exceed the elastic limit.

1. On leave from the Central Research Institute of Electric Power Industry of Japan.

In the last two decades, many control algorithms and devices have been proposed for civil engineering applications (Soong 1990; Housner, *et al*. 1994; Soong and Constantinou 1994; Fujino, *et al*. 1996; Housner, *et al.* 1997; Spencer and Sain 1997), each of which has certain advantages, depending on the specific application and the desired objectives. The seismic response of nonlinear structures to severe earthquakes has also been studied and control algorithms for these nonlinear structures have been proposed by a number of researchers (Masri, *et al*. 1981; Masri, *et al*. 1982; Reinhorn, *et al*. 1987; Yang, *et al*. 1992; Yang, *et al*. 1994; Yang, *et al*. 1995; Pantelides and Nelson 1995; Chang, *et al*. 1996; Bani-Hani and Ghaboussi 1998; Tsai, *et al*. 1998; Barrosa 1999). It is evident that different researchers use different structures and different criteria to show the efficacy and effectiveness of their own particular control strategies. At the present time, structural control research, as a whole, is greatly diversified with regard to these specific applications and desired objectives. A common basis for the comparison of various algorithms and devices does not currently exist. Determination of the general effectiveness of structural control algorithms and devices, a task which is necessary to focus future structural control research and development, is challenging.

Ideally, each proposed control strategy should be evaluated experimentally under conditions that closely model the as-built environment. However, it is impractical, both financially and logistically, for all researchers in structural control to conduct even small-scale experimental tests. An available alternative, denoted “software testbeds” by Caughey (1998), is the use of consensus-approved, high-fidelity, analytical benchmark models to allow researchers in structural control to test their algorithms and devices and to directly compare the results.

The American Society of Civil Engineers (ASCE) Committee on Structural Control has recognized the significance of structural control benchmark problems. The Committee developed a benchmark study, focusing primarily on the comparison of structural control algorithms for three-story building models. The initial results of this study were reported at the 1997 ASCE Structures Congress, held in Portland, Oregon (Spencer, *et al*. 1997; Balas 1997; Lu and Skelton 1997; Wu, *et al*. 1997; Smith, *et al*. 1997). Additionally, a more extensive analysis of these benchmark structural control problems formed the basis for a special issue of *Earthquake Engineering and Structural Dynamics* (Spencer, *et al*. 1998 a, b). Several of these algorithms have been experimentally verified at the University of Notre Dame’s Structural Dynamics and Control/Earthquake Engineering Laboratory (Baker, *et al*. 1999).

Building on the foundation laid by the ASCE Committee on Structural Control, the next generation of benchmark structural control studies were initiated by the Working Group on Building Control during the Second International Workshop on Structural Control held December 18–20, 1996, in Hong Kong (Chen 1996). As stated by the Working Group, the goal of this effort was to develop benchmark models to provide systematic and standardized means by which competing control strategies, including devices, algorithms, sensors, *etc*., can be evaluated. This goal drives the next generation of structural control benchmark problems, and its achievement will take the structural control community another step toward more readily allowing implementation of innovative control strategies for dynamic hazard mitigation.

As an outgrowth of the workshop in Hong Kong, two benchmark problems for the control of buildings were developed for presentation at the 2nd World Conference on Structural Control held June 28–July 1, 1998, in Kyoto, Japan. The first, detailed in Yang, *et al*. (1999), proposed a benchmark problem for wind excited buildings. The second benchmark problem, detailed in Spencer, *et al*. (1999), was the next generation benchmark control problem for seismically excited buildings. These two benchmark studies were successful, although the structural models were considered to

remain perfectly elastic. Large magnitude earthquakes can, however, cause material yielding in the structural elements of civil structures, resulting in nonlinear responses. At the First World Conference on Structural Control held in Pasadena, the necessity of taking into account structural nonlinearity was identified. During the 2nd World Conference on Structural Control, as a result of the success of the linear benchmarks presented, it was decided to pursue a nonlinear analysis.

The benchmark problem presented herein is an extension of the seismically excited next generation benchmark problem presented at the 2nd World Conference on Structural Control to include nonlinear responses and to address other building heights. For this nonlinear benchmark study, 3-, 9- and 20-story steel buildings designed for the SAC[2] project are the benchmark structures considered. Descriptions of these structures are discussed in the next section. High-fidelity nonlinear models of the structures are developed and are designated as the nonlinear evaluation models. In the context of this study, the evaluation models are considered to be true models of the structural systems. Several evaluation criteria, measuring the effectiveness of the control strategies to reduce undesired responses of the evaluation model to ground excitation, are given, along with the associated control design constraints. Researchers/designers participating in this benchmark study can propose control strategies for any of the three benchmark buildings and shall define (including sensors and control algorithms), evaluate and report the results of their proposed control strategies for each building considered. The location on the structure must be specified for each control device and sensor employed. Passive, active and semi-active devices, or a combination thereof, may be considered. Although the dynamics of the control actuators are important to the control design problem (Dyke, *et al*. 1995), for this initial nonlinear benchmark problem, the dynamics of control devices are not considered. Appropriate models for sensors must be identified. For active and semi-active control strategies, control algorithms must also be specified. For illustrative purposes, a complete sample control design, similar to that employed in the next generation benchmark study, is presented for the 20-story benchmark building. Although this sample control system is not intended to be competitive, it demonstrates how one might identify the sensors and control devices employed, build a design model, develop a controller and evaluate a complete control system design.

Benchmark Structures

The 3-, 9- and 20-story structures used for this benchmark study were designed by Brandow & Johnston Associates[3] for the SAC Phase II Steel Project. Although not actually constructed, these structures meet seismic code and represent typical low-, medium- and high-rise buildings designed for the Los Angeles, California region. These buildings were chosen because they also serve as benchmark structures for the SAC studies and, thus, will provide a wider basis for the comparison of results. The specifications for each of these buildings are discussed in the following paragraphs.

---

2. SAC is a joint venture of three non-profit organizations: The Structural Engineers Association of California (SEAOC), the Applied Technology Council (ATC) and California Universities for Research in Earthquake Engineering (CUREE). SAC Steel Project Technical Office, 1301 S. 46th Street, Richmond, CA 94804-4698. http://quiver.eerc.berkeley.edu:8080/.
3. Brandow & Johnston Associates, Consulting Structural Engineers, 1660 W. Third St., Los Angeles, CA 90017.

3-Story Benchmark Building

The three-story (3-story) benchmark structure is 36.58 m (120 ft) by 54.87 m (180 ft) in plan, and 11.89 m (39 ft) in elevation. The bays are 9.15 m (30 ft) on center, in both directions, with four bays in the north-south (N-S) direction and six bays in the east-west (E-W) direction. The building's lateral load-resisting system is comprised of steel perimeter moment-resisting frames (MRFs) with simple framing between the two furthest south E-W frames. The interior bays of the structure contain simple framing with composite floors.

The columns are 345 MPa (50 ksi) steel. The columns of the MRF are wide-flange. The levels of the 3-story building are numbered with respect to the ground level (see Figure 1). The 3rd level is the roof. Typical floor-to-floor heights (for analysis purposes measured from center-of-beam to center-of-beam) are 3.96 m (13 ft). The column bases are modeled as fixed (at the ground level) to the ground.

The floors are composite construction (*i.e.*, concrete and steel). The floor system is comprised of 248 MPa (36 ksi) steel wide-flange beams acting compositely with the floor slab. In accordance with common practice, the floor system, which provides diaphragm action, is assumed to be rigid in the horizontal plane. The inertial effects of each level are assumed to be carried evenly by the floor diaphragm to each perimeter MRF, hence each frame resists one half of the seismic mass associated with the entire structure.

The seismic mass of the structure is due to various components of the structure, including the steel framing, floor slabs, ceiling/flooring, mechanical/electrical, partitions, roofing and a penthouse located on the roof. The seismic mass of the first and second levels is 9.57×10^5 kg (65.5 kips-sec^2/ft) and the third level is 1.04×10^6 kg (71.0 kips-sec^2/ft). The seismic mass of the entire structure is 2.95×10^6 kg (202 kips-sec^2/ft). The 3-story N-S MRF is depicted in Figure 1.

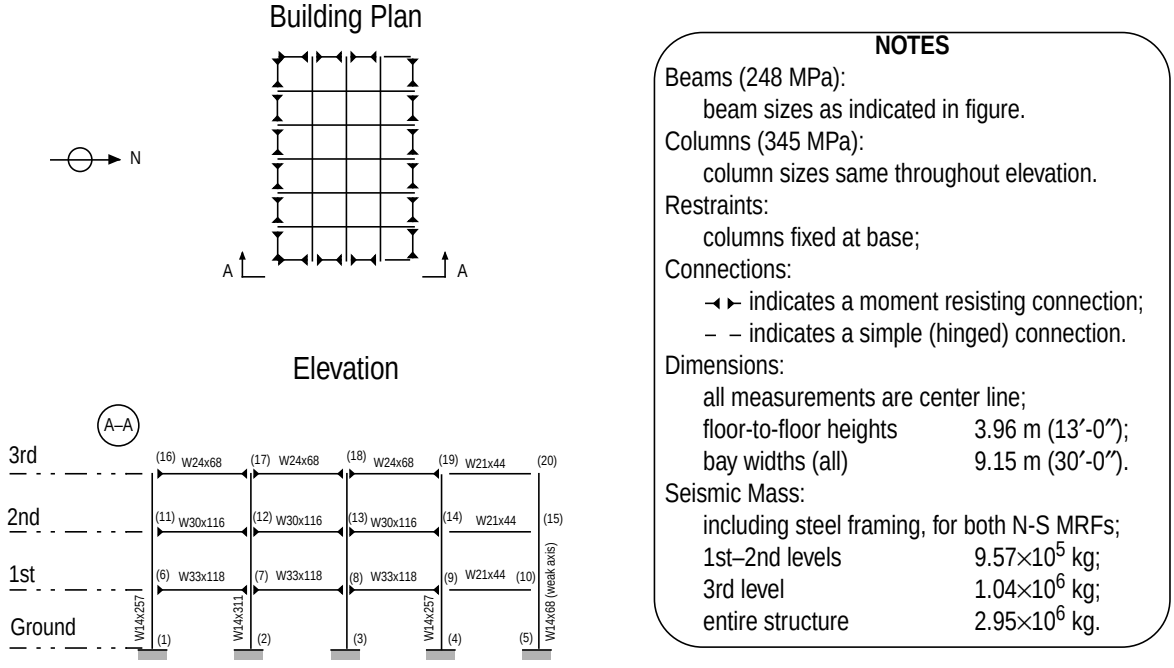

Figure 1. 3-Story Benchmark Building N-S MRF.

9-Story Benchmark Building

The nine-story (9-story) benchmark structure is 45.73 m (150 ft) by 45.73 m (150 ft) in plan, and 37.19 m (122 ft) in elevation. The bays are 9.15 m (30 ft) on center, in both directions, with five bays each in the north-south (N-S) and east-west (E-W) directions. The building's lateral load-resisting system is comprised of steel perimeter moment-resisting frames (MRFs) with simple framing on the furthest south E-W frame. The interior bays of the structure contain simple framing with composite floors.

The columns are 345 MPa (50 ksi) steel. The columns of the MRF are wide-flange. The levels of the 9-story building are numbered with respect to the ground level (see Figure 2). The ninth level is the roof. The building has a basement level denoted B-1. Typical floor-to-floor heights (for analysis purposes measured from center-of-beam to center-of-beam) are 3.96 m (13 ft). The floor-to-floor height of the basement level is 3.65 m (12 ft) and for the first floor is 5.49 m (18 ft).

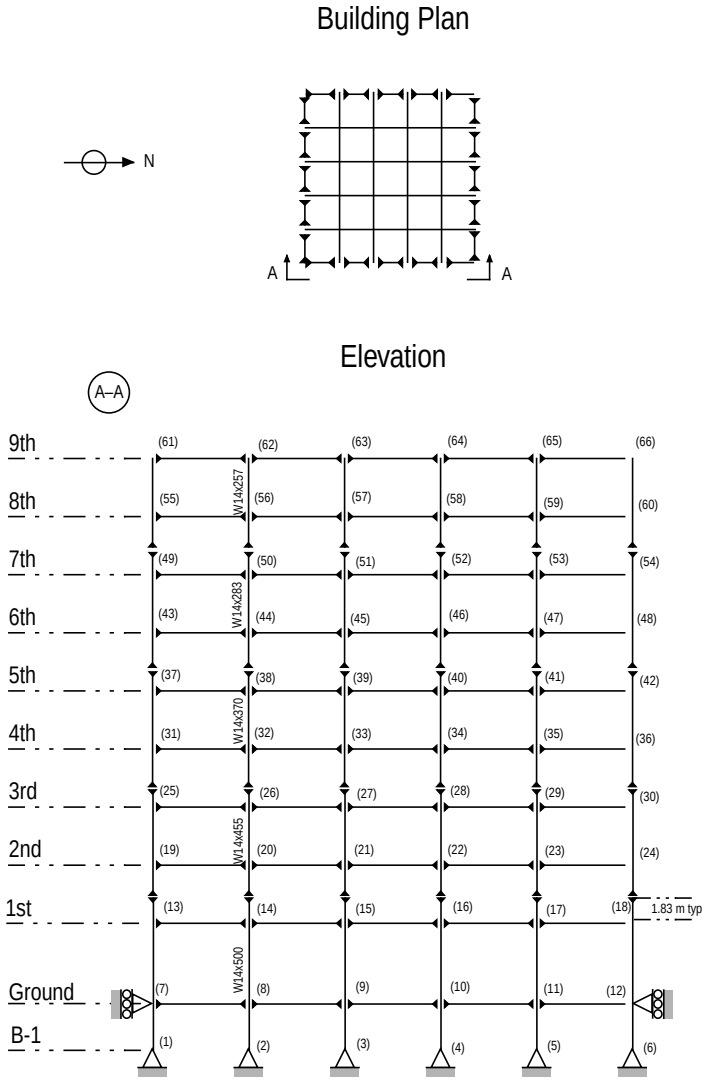

NOTES

Beams (248 MPa):
- Ground– 2nd level W36x160;
- 3rd – 6th level W36x135;
- 7th level W30x99;
- 8th level W27x84;
- 9th level W24x68.

Columns (345 MPa):
- column sizes change at splices
- corner columns and interior columns the same, respectively, throughout elevation;

Restraints:
- columns pinned at base;
- structure laterally restrained at 1st level.

Splices:
- denoted with ⇣⇡;
- are at 1.83 m (6 ft) w.r.t. beam-to-column joint

Connections:
- ⊣⊢ indicates a moment resisting connection.
- – – indicates a simple (hinged) connection.

Dimensions:
- all measurements are center line;
- basement level height 3.65 m (12′-0″);
- Ground level height 5.49 m (18′-0″);
- 1st – 8th level heights 3.96 m (13′-0″);
- bay widths (all) 9.15 m (30′-0″).

Seismic Mass:
- including steel framing, for both N-S MRFs;
- Ground level 9.65×10^5 kg;
- 1st level 1.01×10^6 kg;
- 2nd – 8th level 9.89×10^5 kg;
- 9th level 1.07×10^6 kg;
- entire structure (above ground) 9.00×10^6 kg.

Figure 2. 9-Story Benchmark Building N-S MRF.

The column lines employ two-tier construction, *i.e.* monolithic column pieces are connected every two levels beginning with the first level. Column splices, which are seismic (tension) splices to carry bending and uplift forces, are located on the first, third, fifth and seventh levels at 1.83 m (6 ft) above the center-line of the beam to column joint. The column bases are modeled as pinned and secured to the ground (at the B-1 level). Concrete foundation walls and surrounding soil are assumed to restrain the structure at the ground level from horizontal displacement.

The floor system is comprised of 248 MPa (36 ksi) steel wide-flange beams acting compositely with the floor slab as in the 3-story building. Similar to the 3-story building, each frame resists one half of the seismic mass associated with the entire structure.

The seismic mass of the structure is due to various components of the structure, including the steel framing, floor slabs, ceiling/flooring, mechanical/electrical, partitions, roofing and a penthouse located on the roof. The seismic mass of the ground level is 9.65×10^5 kg (66.0 kips-sec^2/ft), for the first level is 1.01×10^6 kg (69.0 kips-sec^2/ft), for the second through eighth levels is 9.89×10^5 kg (67.7 kips-sec^2/ft) and for the ninth level is 1.07×10^6 kg (73.2 kips-sec^2/ft). The seismic mass of the above ground levels of the entire structure is 9.00×10^6 kg (616 kips-sec^2/ft). The 9-story N-S MRF is depicted in Figure 2.

20-Story Benchmark Building

The twenty-story (20-story) benchmark structure is 30.48 m (100 ft) by 36.58 m (120 ft) in plan, and 80.77 m (265 ft) in elevation. The bays are 6.10 m (20 ft) on center, in both directions, with five bays in the north-south (N-S) direction and six bays in the east-west (E-W) direction. The building's lateral load-resisting system is comprised of steel perimeter moment-resisting frames (MRFs). The interior bays of the structure contain simple framing with composite floors.

The columns are 345 MPa (50 ksi) steel. The interior columns of the MRF are wide-flange. The corner columns are box columns. The levels of the 20-story building are numbered with respect to the ground level (see Figure 3). The building has two basement levels. The level directly below the ground level is the second basement (B-1). The level below B-1 is the second basement (B-2). Typical floor-to-floor heights (for analysis purposes measured from center-of-beam to center-of-beam) are 3.96 m (13 ft). The floor-to-floor heights for the two basement levels are 3.65 m (12 ft) and for the ground level is 5.49 m (18 ft).

The column lines employ three-tier construction, *i.e.* monolithic column pieces are connected every three levels beginning with the first level. Column splices, which are seismic (tension) splices to carry bending and uplift forces, are located on the first, fourth, seventh, tenth, thirteenth, sixteenth and eighteenth levels at 1.83 m (6 ft) above the center-line of the beam to column joint. The column bases are modeled as pinned and secured to the ground (at the B-2 level). Concrete foundation walls and surrounding soil are assumed to restrain the structure at the ground level from horizontal displacement.

The floor system is comprised of 248 MPa (36 ksi) steel wide-flange beams acting compositely with the floor slab as in the 3-story building. Similar to the 3-story building, each frame resists one half of the seismic mass associated with the entire structure.

The seismic mass of the structure is due to various components of the structure, including the steel framing, floor slabs, ceiling/flooring, mechanical/electrical, partitions, roofing and a penthouse located on the roof. The seismic mass, including both N-S MRFs, of the ground level is 5.32×10^5 kg (36.4 kips-sec^2/ft), for the first level is 5.63×10^5 kg (38.6 kips-sec^2/ft), for the second level to 19th level is 5.52×10^5 kg (37.8 kips-sec^2/ft), and for the 20th level is 5.84×10^5 kg (40.0 kips-sec^2/ft). The seismic mass of the above ground levels of the entire structure is 1.11×10^7 kg (760 kips-sec^2/ft). The 20-story N-S MRF is depicted in Figure 3.

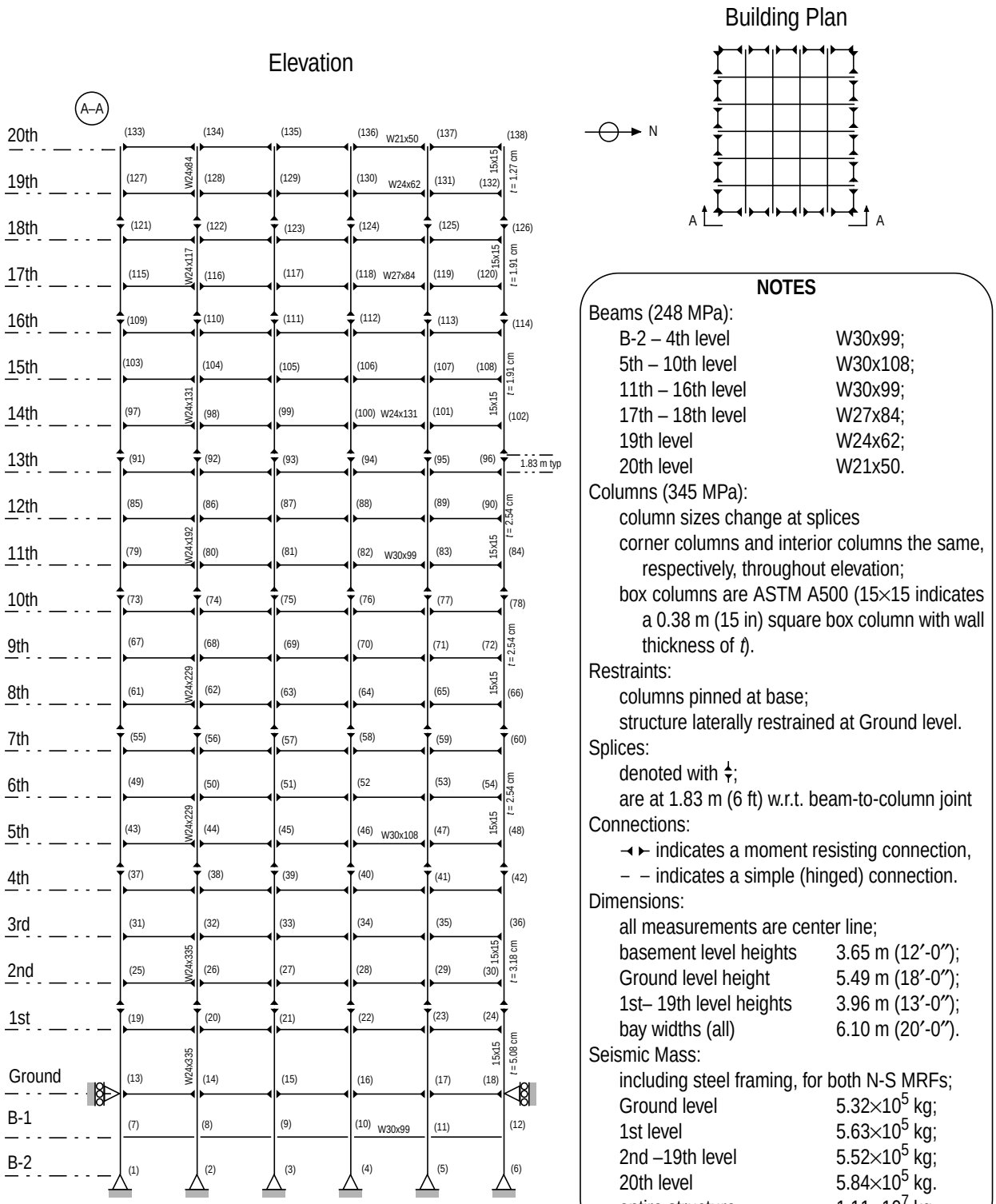

NOTES

Beams (248 MPa):

B-2 – 4th level	W30x99;
5th – 10th level	W30x108;
11th – 16th level	W30x99;
17th – 18th level	W27x84;
19th level	W24x62;
20th level	W21x50.

Columns (345 MPa):

- column sizes change at splices
- corner columns and interior columns the same, respectively, throughout elevation;
- box columns are ASTM A500 (15×15 indicates a 0.38 m (15 in) square box column with wall thickness of *t*).

Restraints:

- columns pinned at base;
- structure laterally restrained at Ground level.

Splices:

- denoted with ⊥;
- are at 1.83 m (6 ft) w.r.t. beam-to-column joint

Connections:

- ⊣ ⊢ indicates a moment resisting connection,
- – – indicates a simple (hinged) connection.

Dimensions:

- all measurements are center line;

basement level heights	3.65 m (12′-0″);
Ground level height	5.49 m (18′-0″);
1st– 19th level heights	3.96 m (13′-0″);
bay widths (all)	6.10 m (20′-0″).

Seismic Mass:

- including steel framing, for both N-S MRFs;

Ground level	5.32×10^5 kg;
1st level	5.63×10^5 kg;
2nd –19th level	5.52×10^5 kg;
20th level	5.84×10^5 kg.
entire structure (above ground)	1.11×10^7 kg.

Figure 3. 20-Story Benchmark Building N-S MRF.

Evaluation Models

This benchmark study will focus on an in-plane (2-D) analysis of the benchmark structures. The frames considered in the development of the evaluation models are the N-S MRFs (the short, or weak, direction of the buildings) for the structures described in the previous section. Passive, active and/or semi-active control devices can be implemented throughout these N-S frames of the 3-, 9- and 20-story structures and their performance assessed using the evaluation models in this section and the evaluation criteria identified in the Control Design section.

Based on the physical description of the 3-, 9- and 20-story structures described in the previous section, in-plane finite element models of the N-S MRFs have been developed. Structural member nonlinearities are included to capture the inelastic behavior of buildings during strong earthquakes. The beams and columns of the structures are modeled as plane-frame elements, and mass and stiffness matrices for each of the structures are determined. A bilinear hysteresis model is used to characterize the nonlinear bending stiffness of the structural members. The damping matrix is determined based on an assumption of Rayleigh damping. This process is described in further detail in the following paragraphs.

Nodes are located at beam-to-column joints. Elements are created between nodes to represent the beams and columns in the structure. The beam members extend from the center-line of column to center-line of column, thus ignoring the column panel zone. Inertial loads, accounting for the seismic mass of the floor slabs, ceiling/flooring, mechanical/electrical, partitions, roofing and penthouse are uniformly distributed at the nodes of each respective level assuming a lumped mass formulation.

The 9- and 20-story building frames contain column splices. The column joint of the splice story is located 1.83 m (6 ft) above the center-line of the beam. For simplicity the spliced columns are modeled as having uniform properties over the story height equal to the weighted average of the upper and lower column properties of that story. There is no node modeled at the splice.

Each node has three degrees-of-freedom (DOFs): horizontal, vertical and rotational. The 3-, 9- and 20-story structures have 60, 198, and 414 DOFs prior to application of boundary conditions/constraints, respectively. Global DOF n is the p-th local DOF (*i.e.*, horizontal: p=1, vertical: p=2, rotational: p=3) of the q-th node, which is indicated in the figures of the previous section, and is given by $n = 3(q-1) + p$.

Each element, modeled as a plane frame element, contains two nodes and six DOFs. The length, area, moment of inertia, modulus of elasticity and mass density are pre-defined for each element. The elemental lumped mass and stiffness matrices are determined as functions of these properties (Sack 1989; Cook, *et al*. 1989). Global mass and stiffness matrices are assembled from the elemental mass and stiffness matrices by summing the mass and stiffness associated with each DOF for each element of the entire structure. Rotational inertia is ignored; thus, rotational mass is assigned a small value. The DOFs corresponding to fixed boundary conditions are then constrained by eliminating the rows and columns associated with these DOFs from the global mass and stiffness matrices.

The simulation of the benchmark buildings is developed to represent control of the entire structure, including both N-S MRFs and the entire mass of each structure. Researchers/designers should recognize that the control strategies applied within this study represent the structural control of the entire benchmark building being considered.

The first three natural frequencies of the 3-story benchmark evaluation model are: 0.99, 3.06, and 5.83 Hz. The first five natural frequencies of the 9-story benchmark evaluation model are: 0.443, 1.18, 2.05, 3.09, and 4.27 Hz. The first 10 natural frequencies of the 20-story bench-

mark evaluation model are: 0.261, 0.753, 1.30, 1.83, 2.40, 2.44, 2.92, 3.01, 3.63 and 3.68 Hz. These results are consistent with those found by others who have modeled this structure (Barrosa 1999; Spencer, *et al*. 1998).

Assuming the structures respond in the elastic range, transfer functions for the displacement and absolute acceleration at the top of each building from ground acceleration can be determined. These transfer functions are provided in Figure 4. The first three mode shapes for the 3-, 9- and 20-story building models are shown in Figure 5.

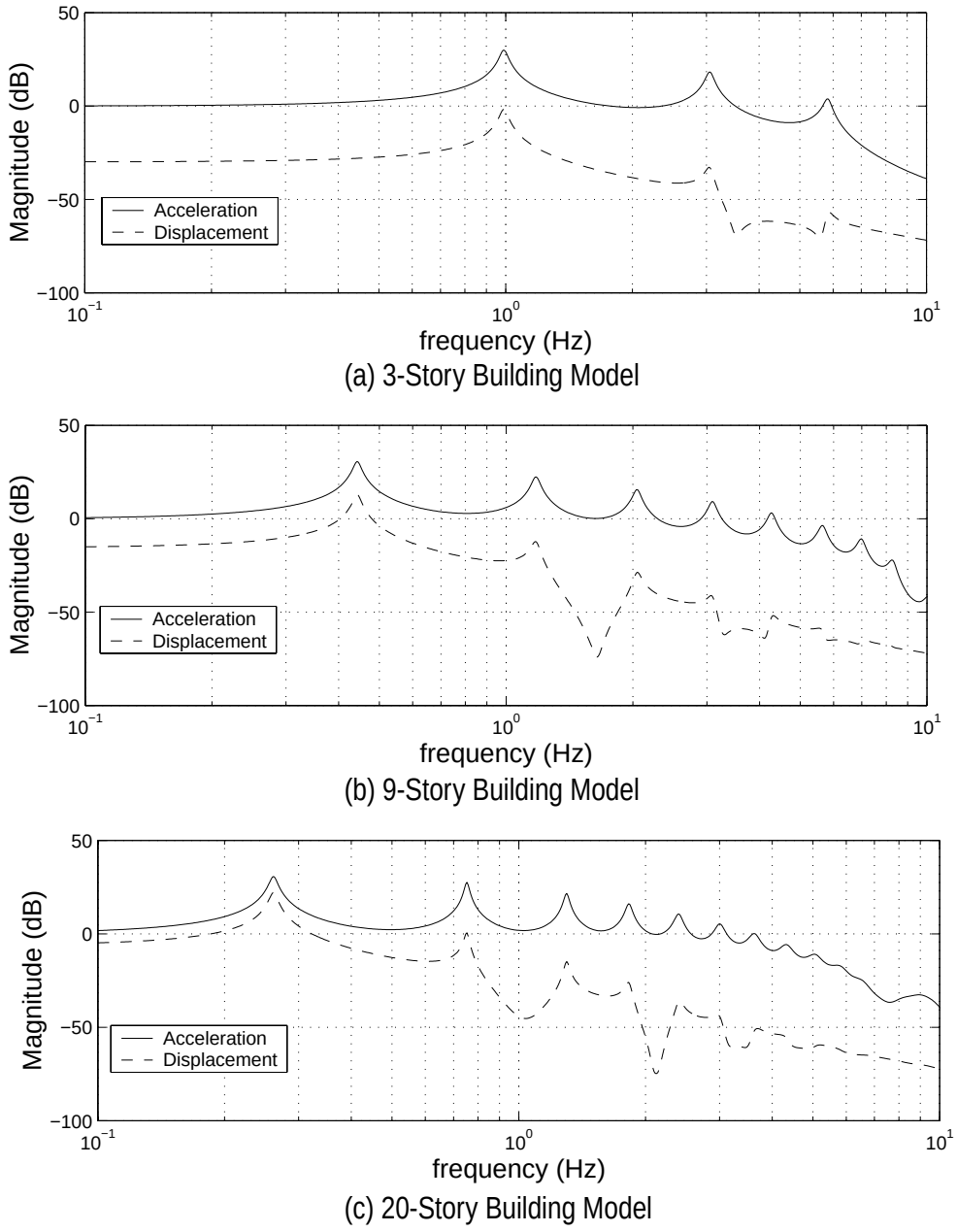

Figure 4. Typical Transfer Functions from Ground Acceleration to Absolute Roof Acceleration (Solid) and Ground Acceleration to Relative Horizontal Roof Displacement (Dashed) for the (a) 3-Story; (b) 9-Story; and (c) 20-Story Building Models.

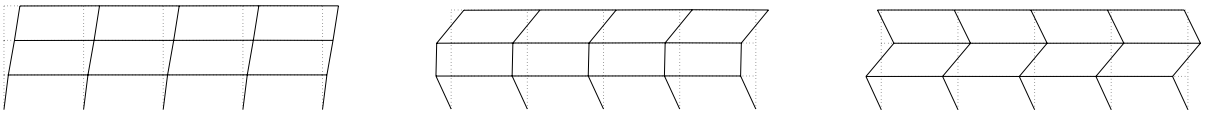

Mode 1 (0.99 Hz) Mode 2 (3.06 Hz) Mode 3 (5.83 Hz)

(a) 3-Story Building Model

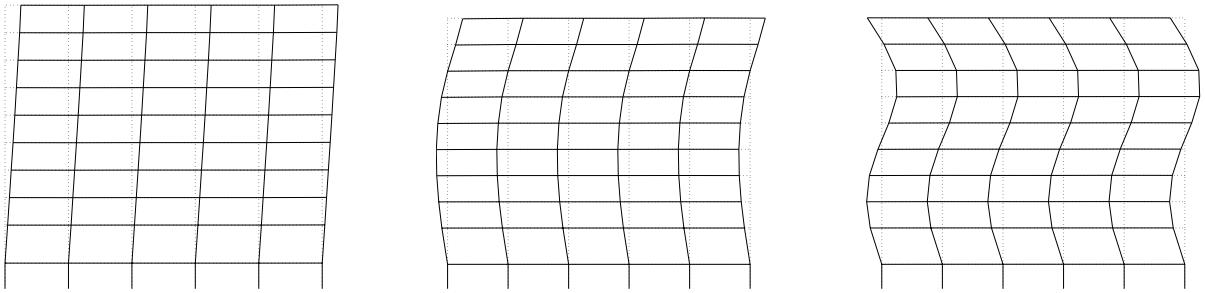

Mode 1 (0.44 Hz) Mode 2 (1.18 Hz) Mode 3 (2.05 Hz)

(b) 9-Story Building Model

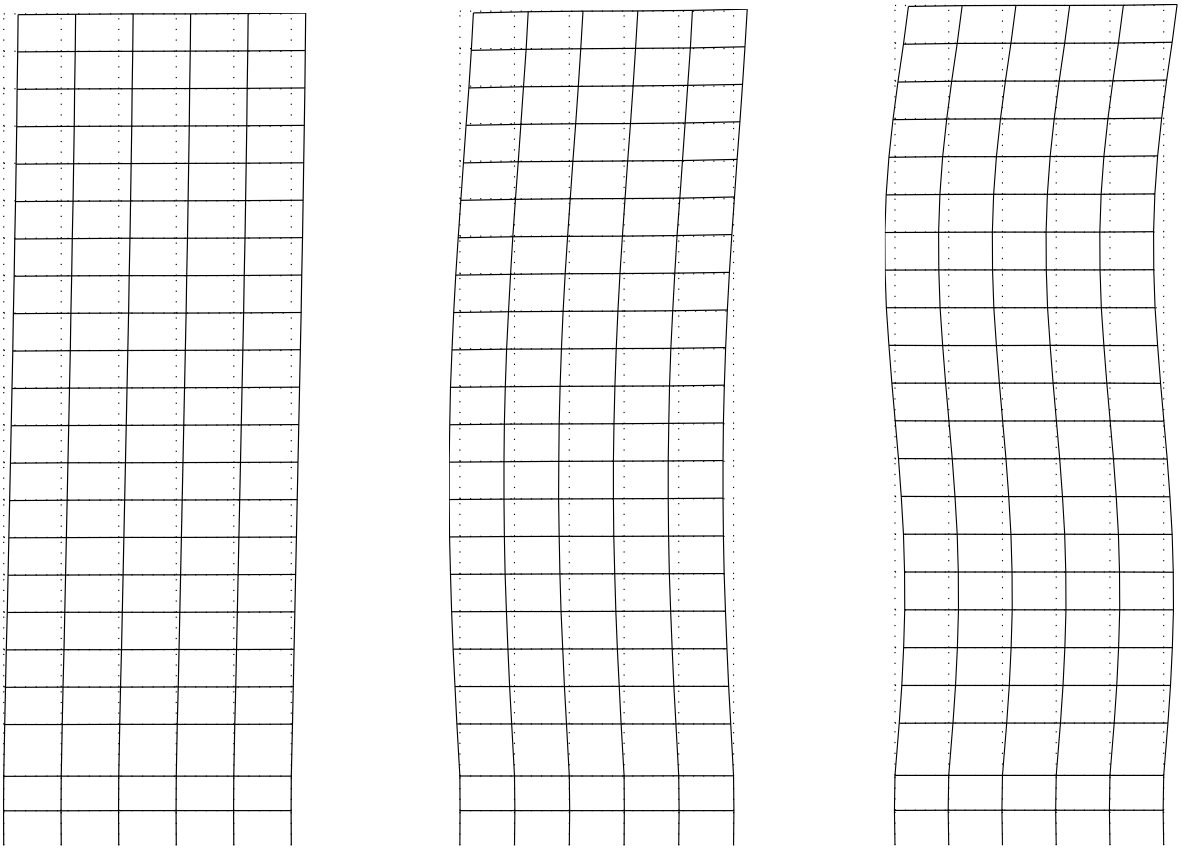

Mode 1 (0.26 Hz) Mode 2 (0.75 Hz) Mode 3 (1.30 Hz)

(c) 20-Story Building Model

Figure 5. Mode Shapes for the (a) 3-Story; (b) 9-Story; and (c) 20-Story Building Models.

Nonlinear Analysis Tool

During large seismic events, structural members can yield, resulting in nonlinear response behavior that may be significantly different than a linear approximation. To better represent the nonlinear behavior, a bilinear hysteresis model, as shown in Figure 6, is used to model the plastic hinges, the points of yielding, of the 3-, 9- and 20-story building structural members. The bilinear bending properties are predefined for each structural member. These plastic hinges, which are assumed to occur at the moment resisting column-beam and column-column connections, introduce a material nonlinear behavior of these structures. While MATLAB® (1997) has a wide range of numerical tools for control design and analysis, it does not have built-in integration schemes that can effectively determine the time domain response of such nonlinear structures. Therefore, an efficient implementation of the Newmark-β time-step integration method was developed in MATLAB for this purpose (Ohtori and Spencer 1999). This section discusses the nonlinear algorithm and its implementation.

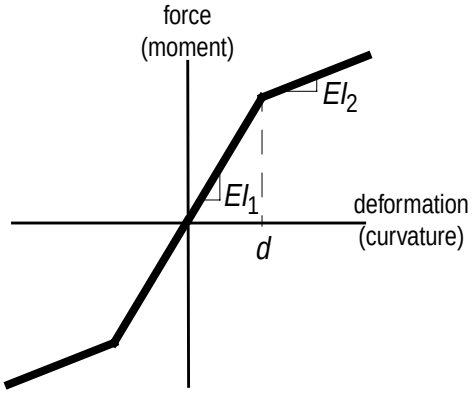

Figure 6. Bilinear Hysteresis Model for Structural Member Bending.

The Newmark-β method, which is reviewed in detail by Subbaraj and Dokainish (1989), is used to solve the incremental equations of motion. The incremental equations of motion for the nonlinear structural system take the following form

$$\mathbf{M}\Delta\ddot{\mathbf{U}} + \mathbf{C}\Delta\dot{\mathbf{U}} + \mathbf{K}\Delta\mathbf{U} = -\mathbf{M}\mathbf{G}\Delta\ddot{x}_g + \mathbf{P}\Delta\mathbf{f} + \Delta\mathbf{F}_{err} \tag{1}$$

where, $\mathbf{M}$, $\mathbf{C}$, and $\mathbf{K}$ are the mass, damping and stiffness matrices of the building, $\Delta\mathbf{U}$ is the incremental response vector, $\mathbf{G}$ is a loading vector for the ground acceleration, $\Delta\ddot{x}_g$ is the ground acceleration increment, $\mathbf{P}$ is a loading vector for the control forces, $\Delta\mathbf{f}$ is the incremental control force and $\Delta\mathbf{F}_{err}$ is the vector of the unbalanced forces. The unbalanced force is the difference between the restoring force evaluated using the hysteresis model and the restoring force assuming constant linear stiffness at time t during the time interval $(t, t + \Delta t)$. This unbalanced force is handled at the next time step. That is, the unbalanced force is added as external force at the next time step.

Because the floor slab is assumed to be rigid in the horizontal plane, the nodes associated with each level have the same horizontal displacements. Therefore, the dependent (slave) horizontal DOFs on each floor slab can be expressed in terms of a single active horizontal DOF. That is, the displacements $\Delta\mathbf{U}$ can be expressed using those of the active nodes, $\Delta\mathbf{U}_{act}$, that include all vertical, all rotational and one horizontal DOF per level. This relation can be written as

$$\Delta\mathbf{U} = \begin{Bmatrix} \Delta\mathbf{U}_{act} \\ \Delta\mathbf{U}_{slv} \end{Bmatrix} = \mathbf{T}_R \Delta\mathbf{U}_{act} \tag{2}$$

in which $\mathbf{T}_R$ is a transformation matrix for expressing the full response vector in terms of the active degrees of freedom.

The reduced damping matrix, $\hat{\mathbf{C}}$, can now be determined using an assumption of Rayleigh damping as

$$\hat{\mathbf{C}} = c_1 \cdot \mathbf{T}_{\mathrm{R}}^{\mathrm{T}} \mathbf{M} \mathbf{T}_{\mathrm{R}} + c_2 \cdot \mathbf{T}_{\mathrm{R}}^{\mathrm{T}} \mathbf{K} \mathbf{T}_{\mathrm{R}} \tag{3}$$

where c_1 and c_2 are chosen such that modal damping coefficients $\zeta_1 = \zeta_5 = 0.02$. The damping in each mode, according to Rayleigh damping, is given by

$$\zeta_i = \zeta_1(\omega_1\omega_5 + \omega_i^2)/(\omega_i\omega_1 + \omega_5^2) \tag{4}$$

where ω_i is the natural frequency of the *i*-th mode. A plot of the damping coefficients in the respective modes for the 20-story building model is shown in Figure 7.

The following two expressions, proposed by Newmark (1959), are employed to solve the incremental equations of motion in Eq. (1):

$$\mathbf{U}_{t+\Delta t} = \mathbf{U}_t + \Delta t \dot{\mathbf{U}}_t + (\Delta t)^2 \left[\left(\frac{1}{2} - \beta \right) \ddot{\mathbf{U}}_t + \beta \ddot{\mathbf{U}}_{t+\Delta t} \right] \tag{5}$$

$$\dot{\mathbf{U}}_{t+\Delta t} = \dot{\mathbf{U}}_t + \Delta t [(1-\gamma)\ddot{\mathbf{U}}_t + \gamma \ddot{\mathbf{U}}_{t+\Delta t}] \tag{6}$$

in which Δt is the calculation time interval, $\{\ \}_{t+\Delta t}$ and $\{\ \}_t$ are the responses at $t + \Delta t$ and t, respectively, and β and γ are the Newmark parameters. When $\beta = 1/4$ and $\gamma = 1/2$, the calculations are unconditionally stable. Substituting Eq. (5) and Eq. (6) into Eq. (1), the following equations can be derived:

$$\mathbf{T}_{\mathrm{R}}{}^{\mathrm{T}} \mathbf{K}_{\mathrm{D}} \mathbf{T}_{\mathrm{R}} \Delta \mathbf{U}_{\mathrm{act}} = \mathbf{T}_{\mathrm{R}}{}^{\mathrm{T}} \Delta \mathbf{F}_{\mathrm{D}} \tag{7}$$

where

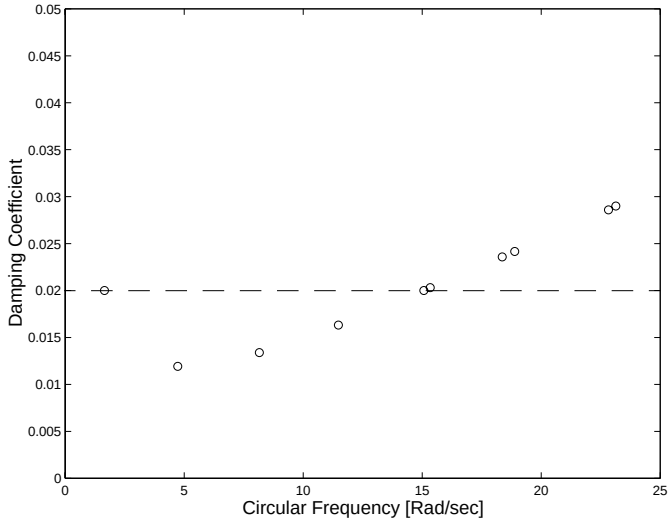

Figure 7. Damping Coefficients for the First 10 Modes of the 20-Story Building.

$$\mathbf{K}_{\mathrm{D}} = \frac{1}{\beta(\Delta t)^2}\mathbf{M} + \frac{\gamma}{\beta\Delta t}\mathbf{C} + \mathbf{K}_t \tag{8}$$

$$\begin{aligned}\Delta\mathbf{F}_{\mathrm{D}} = &-\mathbf{M}\mathbf{G}\Delta\ddot{x}_{\mathrm{g}} + \left(\frac{1}{2\beta}\mathbf{M} + \left(\frac{\gamma}{2\beta} - 1\right)\Delta t\mathbf{C}\right)\ddot{\mathbf{U}}_t \\ &+ \left(\frac{1}{\beta\Delta t}\mathbf{M} + \frac{\gamma}{\beta}\mathbf{C}\right)\dot{\mathbf{U}}_t + \mathbf{P}\Delta\mathbf{F} + \Delta\mathbf{F}_{\mathrm{err}}\end{aligned} \tag{9}$$

$$\mathbf{C} = (\mathbf{T}_{\mathrm{R}}{}^{\mathrm{T}})^{-1}\hat{\mathbf{C}}\mathbf{T}_{\mathrm{R}}{}^{-1} \tag{10}$$

and where $\mathbf{K}_t$ is the tangent (instantaneous) stiffness matrix of the structure at time t.

To determine the tangent stiffness, $\mathbf{K}_t$, a concentrated plasticity model is implemented to model the material nonlinearity of the structural members. The concentrated plasticity model is appropriate for steel structures such as the steel moment resisting frame structures being considered here. The spread plasticity model forms the basis for the concentrated plasticity model. The matrix coefficients of the spread plasticity model were derived by Lobo (1994) and rewritten for improved numerical stability by Valles, *et al*. (1996). These models use a flexural formulation to derive the element stiffnesses of the nonlinear elements. With the concentrated plasticity model (Clough and Johnson 1966; Giberson 1967), the members are assumed to be elastic and yielding occurs only at the ends. The parameters α_{AA} and α_{BB} are introduced so as to express the inelastic spring at the end of each member. For the concentrated plasticity model, the following stiffness matrix is used for expressing the material nonlinearity

$$\begin{Bmatrix} M_{\mathrm{A}} \\ M_{\mathrm{B}} \end{Bmatrix} = \begin{bmatrix} f_{\mathrm{AA}} & f_{\mathrm{AB}} \\ f_{\mathrm{BA}} & f_{\mathrm{BB}} \end{bmatrix}^{-1} \begin{Bmatrix} \theta_{\mathrm{A}} \\ \theta_{\mathrm{B}} \end{Bmatrix} \tag{11}$$

In the Eq. (11), the flexibility coefficients of the elements are:

$$f_{AA} = \frac{L}{12EI_0EI_{\mathrm{A}}EI_{\mathrm{B}}} f_{AA}{}' + \frac{1}{(GA)L} \tag{12}$$

$$f_{AB} = f_{BA} = \frac{L}{12EI_0EI_{\mathrm{A}}EI_{\mathrm{B}}} f_{AB}{}' + \frac{1}{(GA)L} \tag{13}$$

$$f_{BB} = \frac{L}{12EI_0EI_{\mathrm{A}}EI_{\mathrm{B}}} f_{BB}{}' + \frac{1}{(GA)L} \tag{14}$$

where

$$f_{\mathrm{AA}}{}' = 4EI_{\mathrm{A}}EI_{\mathrm{B}} + (EI_0 - EI_{\mathrm{A}})EI_{\mathrm{B}}\alpha_{AA} \tag{15}$$

$$f_{\mathrm{AB}}{}' = -2EI_{\mathrm{A}}EI_{\mathrm{B}} \tag{16}$$

$$f_{\mathrm{BB}}{}' = 4EI_{\mathrm{A}}EI_{\mathrm{B}} + (EI_0 - EI_{\mathrm{B}})EI_{\mathrm{A}}\alpha_{BB} \tag{17}$$

in which M_A and M_B are the moments at the ends A and B of the element, respectively; θ_A and θ_B are the rotations at the ends A and B; EI_A and EI_B are flexural stiffness at the ends of the members at A and B, respectively; EI_0 is the center stiffness of the member; GA is the shear stiffness of the member; and L is the length of the member.

MATLAB Implementation of Nonlinear Analysis

The nonlinear evaluation model requires a MATLAB-based program, implemented as a SIMULINK® system function (S-function), to calculate the nonlinear response of the model. This S-function performs the nonlinear dynamic analysis using the previously discussed Newmark-β method. The accuracy of the nonlinear evaluation model was verified with the commercial structural analysis program IDARC2D (Ohtori and Spencer 1999).

Control Design

The task of the researchers/designers in the benchmark study control design problems is to define an appropriate passive, active, or semi-active control strategy, or a combination thereof. It is left to the researchers/designers to define the type, appropriate model and location of the control device(s)/sensor(s) and to develop appropriate control algorithms. The evaluation model, however, will remain invariant to the various applied control strategies. By using a specific building model and common evaluation criteria, various control strategies can be compared directly, fulfilling the purpose of these benchmark problems. In this section an overview of the control design process, with respect to the task of the researcher/designer, is offered, and the interface with the various models of the simulation are identified.

Overview of Researcher/Designer Tasks

As part of the MATLAB-based nonlinear benchmark study, four programs and four data sets are employed directly. The data flow between the MATLAB-based programs and data sets is shown in Figure 8. Shaded tasks are predefined and remain invariant to the different control strategies, clear tasks are to be defined by each researcher/designer. Each proposed control strategy requires the researcher/designer to define an input/output data file to identify the input location of control forces onto the evaluation model and the type and location of output responses of the evaluation model for evaluation, measurement and connectivity purposes. Additionally, the researcher/designer must define sensor and controller models for their proposed control strategy. Each proposed control strategy is applied to a nonlinear evaluation model and simulated for seismic excitation. The simulator for the nonlinear evaluation model is illustrated in Figure 9. To run the nonlinear evaluation model simulation, the researcher/designer must include SIMULINK blocks for their sensor(s) and controller/control device(s). The final task of each researcher/designer is to evaluate their proposed control strategy using the evaluation criteria discussed in the following Evaluation Criteria section.

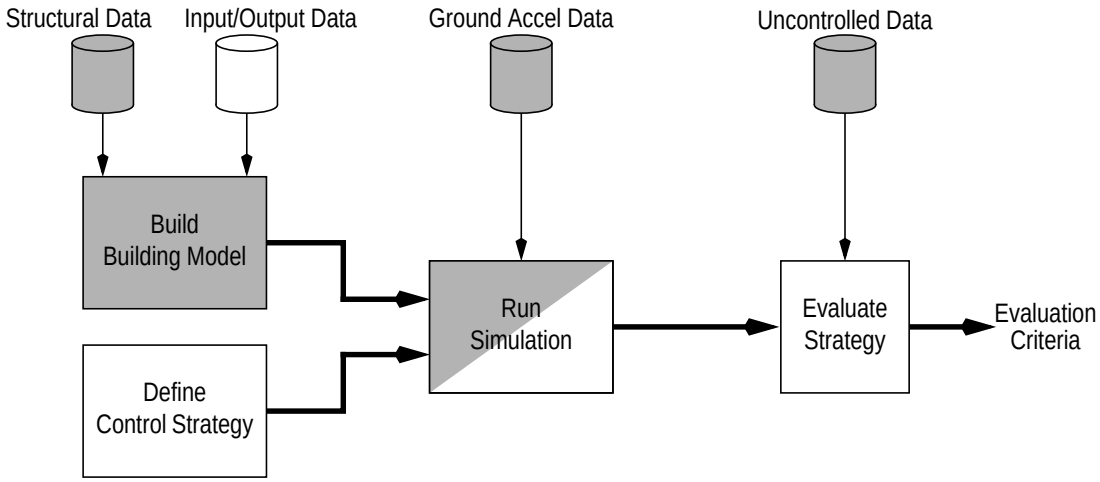

Figure 8. Schematics of the Nonlinear Benchmark Evaluation Model. (Shaded Tasks are Predefined; White Tasks are Defined by Researcher/Designer)

Benchmark Control Problems
for Seismically Excited Nonlinear Buildings

by
Y. Ohtori, R.E. Christenson, B.F. Spencer
and S.J. Dyke

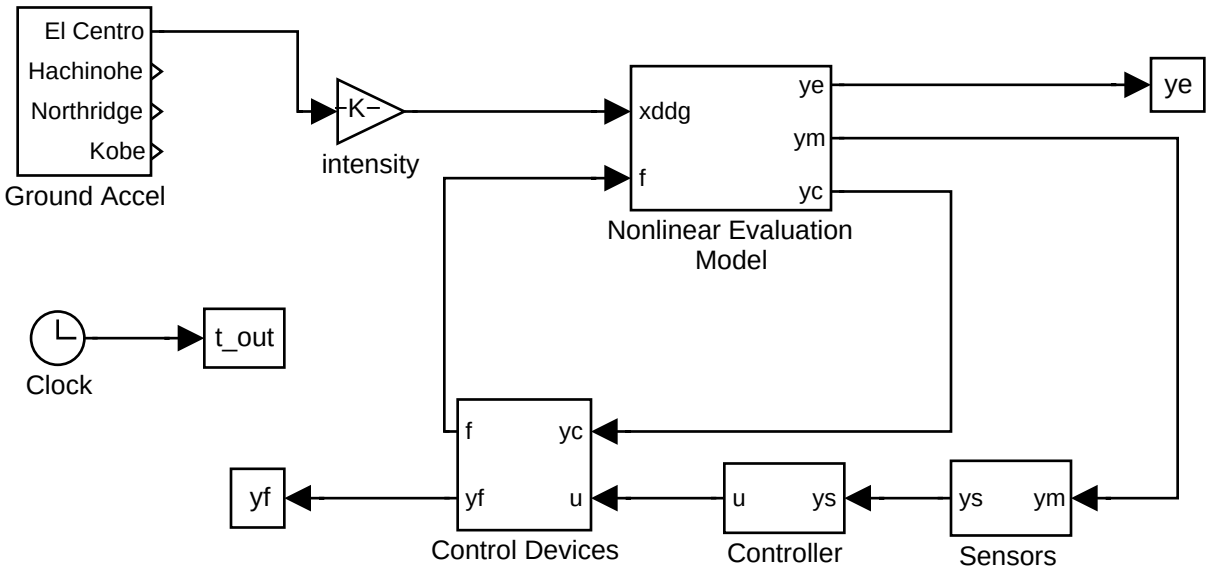

Figure 9. SIMULINK Block Diagram for Vibration Control Simulator.

Interfacing with the Evaluation Model

The evaluation model for the 3-, 9- and 20-story structures takes the general form

$$\dot{\mathbf{x}} = \mathbf{g}_1(\mathbf{x}, \mathbf{f}, \ddot{\mathbf{x}}_g) \tag{18}$$

$$\mathbf{y}_\mathrm{m} = \mathbf{g}_2(\mathbf{x}, \mathbf{f}, \ddot{\mathbf{x}}_g) \tag{19}$$

$$\mathbf{y}_\mathrm{e} = \mathbf{g}_3(\mathbf{x}, \mathbf{f}, \ddot{\mathbf{x}}_g) \tag{20}$$

$$\mathbf{y}_\mathrm{c} = \mathbf{g}_4(\mathbf{x}, \mathbf{f}, \ddot{\mathbf{x}}_g) \tag{21}$$

where $\mathbf{x}$ is the state vector, $\mathbf{y}_\mathrm{m}$ is the vector corresponding to the measured outputs, $\mathbf{y}_\mathrm{e}$ is the vector corresponding to the building response evaluation outputs that are used for evaluation of the system, and $\mathbf{y}_\mathrm{c}$ is the vector of output responses that are used as inputs to control device models. The specific response quantities considered in $\mathbf{y}_\mathrm{m}$, $\mathbf{y}_\mathrm{e}$, and $\mathbf{y}_\mathrm{c}$ should be specified in the user defined data file for outputs. It should be noted here that information regarding the building damage is saved directly by the nonlinear evaluation model and need not be specified in the vector $\mathbf{y}_\mathrm{e}$. Equation (18), in general a nonlinear equation, is solved using the Newmark-β method and the nonlinear evaluation model described previously.

Interfacing with the Sensor Models

For active/semi-active control strategies to interface with the benchmark building model defined in Eqs. (18)-(21), the measured outputs of the evaluation model must be measured by sensors. Researchers/designers should develop models for the sensors which take the form

$$\dot{\mathbf{x}}^\mathrm{s} = \mathbf{g}_5(\mathbf{x}^\mathrm{s}, \mathbf{y}_\mathrm{m}, t) \tag{22}$$

$$\mathbf{y}^\mathrm{s} = \mathbf{g}_6(\mathbf{x}^\mathrm{s}, \mathbf{y}_\mathrm{m}, \mathbf{v}, t) \tag{23}$$

where $\mathbf{x}^\mathrm{s}$ is the continuous time state vector of the sensor(s), $\mathbf{v}$ is a measurement noise vector and $\mathbf{y}^\mathrm{s}$ is the continuous time output of the sensor(s). All measured responses have units of Volts.

Interfacing with the Controller

For active/semi-active control systems, the corresponding controller is required to take the form

$$\mathbf{x}^\mathrm{c}_{k+1} = \mathbf{g}_7(\mathbf{x}^\mathrm{c}_k, \mathbf{y}^\mathrm{s}_k, k) \tag{24}$$

$$\mathbf{u}_k = \mathbf{g}_8(\mathbf{x}^\mathrm{c}_k, \mathbf{y}^\mathrm{s}_k, k) \tag{25}$$

where $\mathbf{x}_k^c$ is the discrete state vector of the control algorithm at time $t = kT$, $\mathbf{y}_k^s$ is the sampled input to the control algorithm (discretized measured output from the sensor model), and $\mathbf{u}_k$ is the discrete control command from the control algorithm.

Interfacing with the Control Device Models

For this initial nonlinear benchmark problem, ideal control actuators may be assumed. The control force and device information would take the form

$$\mathbf{f} = \mathbf{g}_9(\mathbf{y}_c, \mathbf{u}, t) \tag{26}$$

$$\mathbf{y}_f = \mathbf{g}_{10}(\mathbf{y}_c, \mathbf{u}, t) \tag{27}$$

where $\mathbf{f}$ is the continuous time force output (in Newtons) of the control device(s) applied to the structure, $\mathbf{y}_f$ is the vector of control device responses used for evaluation purposes and $\mathbf{u}$ is the continuous controller output (sample and hold of $\mathbf{u}_k$) in Volts.

Evaluation results should be presented for a control strategy using idealized actuators. However, if a researcher/designer wants to include actuator dynamics, to interface with the benchmark building model the control device model(s) should take the form

$$\dot{\mathbf{x}}^a = \mathbf{g}_{11}(\mathbf{x}^a, \mathbf{y}_c, \mathbf{u}, t) \tag{28}$$

$$\mathbf{f} = \mathbf{g}_9(\mathbf{x}^a, \mathbf{y}_c, \mathbf{u}, t) \tag{29}$$

$$\mathbf{y}_f = \mathbf{g}_{10}(\mathbf{x}^a, \mathbf{y}_c, \mathbf{u}, t) \tag{30}$$

where $\mathbf{x}^a$ is the continuous time state vector of the control device. Note that for passive control devices, $\mathbf{g}_9$, $\mathbf{g}_{10}$ and (if applicable) $\mathbf{g}_{11}$ will not be functions of $\mathbf{u}$.

Evaluation Criteria

In order to evaluate proposed control strategies, two far-field and two near-field historical records are selected: (i) *El Centro*. The N-S component recorded at the Imperial Valley Irrigation District substation in El Centro, California, during the Imperial Valley, California earthquake of May 18, 1940. (ii) *Hachinohe*. The N-S component recorded at Hachinohe City during the Tokachi-oki earthquake of May 16, 1968. (iii) *Northridge*. The N-S component recorded at Sylmar County Hospital parking lot in Sylmar, California, during the Northridge, California earthquake of January 17, 1994. (iv) *Kobe*. The N-S component recorded at the Kobe Japanese Meteorological Agency (JMA) station during the Hyogo-ken Nanbu earthquake of January 17, 1995. The absolute peak acceleration of the earthquake records are 3.417, 2.250, 8.2676, and 8.1782 m/sec^2, respectively. The earthquake records are shown in Figure 10.

Additionally, this benchmark study will consider various levels of each of the earthquake records including: 0.5, 1.0 and 1.5 times the magnitude of El Centro and Hachinohe; and 0.5 and 1.0 times the magnitude of Northridge and Kobe. This is a total of 10 earthquake records to be considered in the evaluation of each control strategy.

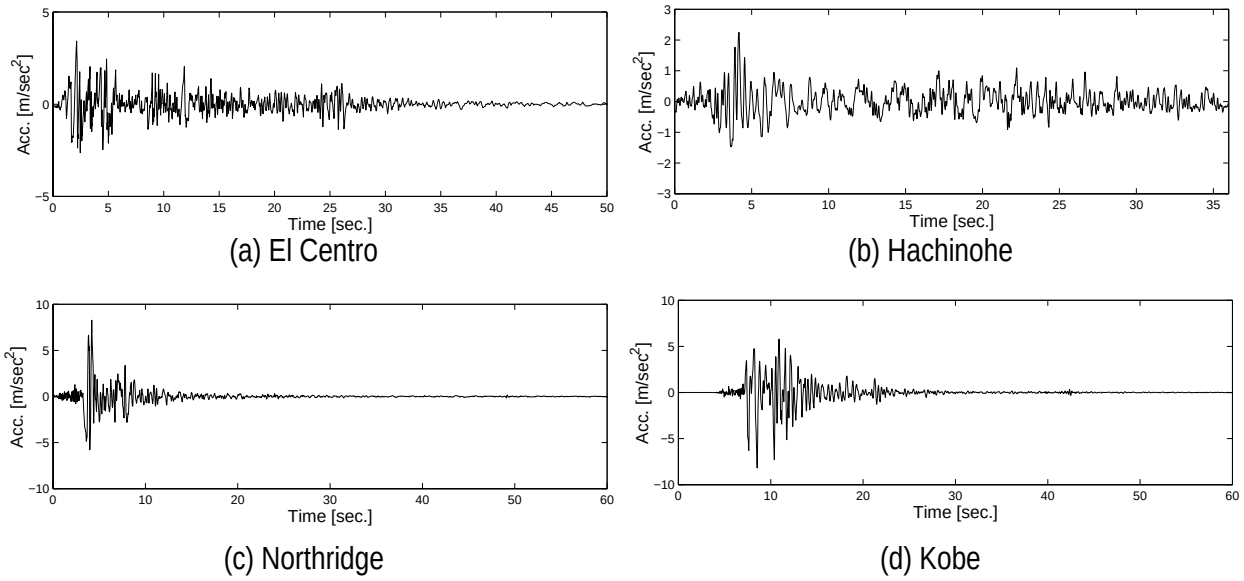

Figure 10. Time Histories of the Near and Far Field Historical Earthquake Records Used in the Benchmark Study: (a) El Centro; (b) Hachinohe; (c) Northridge; and (d) Kobe.

The evaluation criteria are divided into four categories: building responses, building damage, control devices, and control strategy requirements. The first three categories have both peak and normed based criteria. Small values of the evaluation criteria are generally more desirable.

The first category of the evaluation criteria is related to the building responses. The first three criteria are based on peak interstory drift ratio (J_1), level acceleration (J_2) and base shear (J_3):

$$J_1 = \max_{\substack{\text{El Centro}\\ \text{Hachinohe}\\ \text{Northridge}\\ \text{Kobe}}} \left\{ \frac{\max_{t,\,i} \dfrac{|d_i(t)|}{h_i}}{\delta^{\max}} \right\} \tag{31}$$

$$J_2 = \max_{\substack{\text{El Centro}\\ \text{Hachinohe}\\ \text{Northridge}\\ \text{Kobe}}} \left\{ \frac{\max_{t,\,i} |\ddot{x}_{ai}(t)|}{\ddot{x}_{\mathrm{a}}^{\max}} \right\} \tag{32}$$

$$J_3 = \max_{\substack{\text{El Centro}\\ \text{Hachinohe}\\ \text{Northridge}\\ \text{Kobe}}} \left\{ \frac{\max_{t} \left| \sum_i m_i \ddot{x}_{ai}(t) \right|}{F_{\mathrm{b}}^{\max}} \right\} \tag{33}$$

over the range $i = [1, 3]$, $i = [1, 9]$ and $i = [1, 20]$ for the 3-, 9- and 20-story buildings respectively (includes only above ground levels), where $d_i(t)$ is the interstory drift of the above ground level over the time history of each earthquake, h_i is the height of each of the associated

stories, $\delta^{\max}$ is the maximum interstory drift ratio of the uncontrolled structure calculated by equation of $\max_{t,i} |d_i(t)/h_i|$, $\ddot{x}_{ai}(t)$ and $\ddot{x}_{\mathrm{a}}^{\max}$ are absolute acceleration of the *i*-th level with and without control devices respectively, m_i is the seismic mass of the *i*-th above ground level and $F_{\mathrm{b}}^{\max}$ is the maximum base shear of the uncontrolled structure for each respective earthquake.

The next three criteria are based on normed building responses. The interstory drift (J_4), level acceleration (J_5), and base shear (J_6) are defined in their normed based forms as

$$J_4 = \max_{\substack{\text{El Centro}\\ \text{Hachinohe}\\ \text{Northridge}\\ \text{Kobe}}} \left\{ \frac{\max_i \dfrac{\|d_i(t)\|}{h_i}}{\|\delta^{\max}\|} \right\} \tag{34}$$

$$J_5 = \max_{\substack{\text{El Centro}\\ \text{Hachinohe}\\ \text{Northridge}\\ \text{Kobe}}} \left\{ \frac{\max_i \|\ddot{x}_{ai}(t)\|}{\|\ddot{x}_{\mathrm{a}}^{\max}\|} \right\} \tag{35}$$

$$J_6 = \max_{\substack{\text{El Centro}\\ \text{Hachinohe}\\ \text{Northridge}\\ \text{Kobe}}} \left\{ \frac{\left\|\sum_i m_i \ddot{x}_{ai}(t)\right\|}{\|F_{\mathrm{b}}^{\max}\|} \right\} \tag{36}$$

where the norm, $\|\cdot\|$, is computed using the following equation

$$\|\cdot\| \equiv \sqrt{\frac{1}{t_f}\int_0^{t_f} [\cdot]^2 dt} \tag{37}$$

and t_f is a sufficiently large time to allow the response of the structure to attenuate. In this benchmark study the duration of 100 sec is adopted for the El Centro, Hachinohe, and Northridge earthquakes and 180 sec for the Kobe earthquake. The normed values for $\|\delta^{\max}\| \equiv \max_i \|d_i(t)/h_i\|$, $\|\ddot{x}_{\mathrm{a}}^{\max}\|$, and $\|F_{\mathrm{b}}^{\max}\|$ are the maximum normed interstory drift ratio, absolute acceleration and base shear force corresponding to the uncontrolled structure excited by each respective earthquake.

The second category of the evaluation criteria assesses the building damage. These criteria have been added because of the nonlinear character of this benchmark study. Both ends of each element are considered in these criteria to assess the yielding, excluding simply supported beam elements (as well as the fixed-hinged beam elements in the 9-story structure). The seventh and eighth evaluation criteria are based on peak responses while the ninth and tenth are normed-based criteria. The evaluation criteria for the ductility factor (J_7) and dissipated energy of the curvatures at the end of members (J_8) are defined as

$$J_7 = \max_{\substack{\text{El Centro}\\ \text{Hachinohe}\\ \text{Northridge}\\ \text{Kobe}}} \left\{ \frac{\max_{t,j} \dfrac{|\phi_j(t)|}{\phi_{yj}}}{\phi^{\max}} \right\} \tag{38}$$

$$J_8 = \max_{\substack{\text{El Centro}\\ \text{Hachinohe}\\ \text{Northridge}\\ \text{Kobe}}} \left\{ \frac{\max_{t,j} \dfrac{\int dE_j}{F_{yj} \cdot \phi_{yj}}}{E^{\max}} \right\} \tag{39}$$

where ϕ_j is the curvature at the ends of the j-th element (member), $\int dE_j$ is the dissipated energy at the ends of the member during the respective earthquake, ϕ_{yj} and F_{yj} are the yield curvature and the yield moment at the end of the j-th member, respectively, and $\phi^{\max}$ and $E^{\max}$ are the maximum curvatures and the maximum dissipated energy (maximum of all element ends and over time) of uncontrolled structure.

The ninth evaluation criterion (J_9) is the ratio of the plastic connections sustained by the structure while controlled and uncontrolled and is given by

$$J_9 = \max_{\substack{\text{El Centro}\\ \text{Hachinohe}\\ \text{Northridge}\\ \text{Kobe}}} \left\{ \frac{N_d^C}{N_d} \right\} \tag{40}$$

where N_d is the number of damaged connections (member ends) without control and N_d^C are the number of damaged connections with control. Evaluation criteria J_8 and J_9 only have meaning for structures undergoing plastic deformations and are, therefore, undefined (should not be calculated or reported) when the uncontrolled building remains elastic.

The tenth evaluation criterion (J_{10}) is the normed ductility factor and is given by

$$J_{10} = \max_{\substack{\text{El Centro}\\ \text{Hachinohe}\\ \text{Northridge}\\ \text{Kobe}}} \left\{ \frac{\max_{j} \dfrac{\|\phi_j(t)\|}{\phi_{yj}}}{\|\phi^{\max}\|} \right\} \tag{41}$$

where $\|\phi_j(t)\|$ and $\|\phi^{\max}\|$ are the normed curvature at the member ends with and without control, respectively. The curvature (ϕ_j), normed curvature ($\|\phi_j(t)\|$), dissipated energy ($\int dE_j$) and information to determine the number of plastic hinges (N_d) are determined within the nonlinear S-function during the simulation and saved to a specified data file.

The third category is related to the control devices. This category assess the required performance of the devices. Peak criterion J_{11}, J_{12}, and J_{13} show control force, control device stroke, and power used for control

$$J_{11} = \max_{\substack{\text{El Centro}\\ \text{Hachinohe}\\ \text{Northridge}\\ \text{Kobe}}} \left\{ \frac{\max_{t,\,l} \left| f_l(t) \right|}{W} \right\} \tag{42}$$

$$J_{12} = \max_{\substack{\text{El Centro}\\ \text{Hachinohe}\\ \text{Northridge}\\ \text{Kobe}}} \left\{ \frac{\max_{t,\,l} \left| y_l^{\mathrm{a}}(t) \right|}{x^{\max}} \right\} \tag{43}$$

$$J_{13} = \max_{\substack{\text{El Centro}\\ \text{Hachinohe}\\ \text{Northridge}\\ \text{Kobe}}} \left\{ \frac{\max_{t} \left[\sum_{l} \mathcal{P}_l(t) \right]}{\dot{x}^{\max} W} \right\} \tag{44}$$

where $f_l(t)$ is the force generated by the l-th control device over the time history of each earthquake, W is the seismic weight of the building based on the above ground mass of the structure (excluding the mass below or at the ground level), $y_l^{\mathrm{a}}(t)$ is the displacement across the l-th control device during the earthquake, $x^{\max}$ is the maximum uncontrolled displacement of the levels relative to the ground, $\mathcal{P}_l(t)$ is a measure of the instantaneous power required by the l-th control device and $\dot{x}^{\max}$ is the maximum uncontrolled velocity of the levels relative to the ground. For active control devices $\mathcal{P}_l(t) \equiv \left| \dot{y}_l^{\mathrm{a}}(t) f_l(t) \right|$, where $\dot{y}_l^{\mathrm{a}}(t)$ is the velocity across the l-th control device. For semi-active devices $\mathcal{P}_l(t)$ is the actual power required to operate the device. For the passive control devices the power required is zero.

The fourteenth evaluation criterion (J_{14}) is a measure of the total power required for the control of the structure and is defined as

$$J_{14} = \max_{\substack{\text{El Centro}\\ \text{Hachinohe}\\ \text{Northridge}\\ \text{Kobe}}} \left\{ \frac{\sum_{l} \frac{1}{t_f} \int_0^{t_f} \mathcal{P}_l(t)}{\dot{x}^{\max} W} \right\} \tag{45}$$

With passive control devices, the J_{14} criterion is zero.

The last category for evaluating the performance is related to the control strategy of each method. The fifteenth (J_{15}), sixteenth (J_{16}) and seventeenth (J_{17}) evaluation criteria are

$$J_{15} = \text{Number of control devices} \tag{46}$$

$$J_{16} = \text{Number of required sensors} \tag{47}$$

$$J_{17} = \dim(\mathbf{x}_k^{\mathrm{c}}) \tag{48}$$

The J_{15} criterion is the total number of control devices implemented to control the benchmark building. The J_{16} criterion is the total number of control sensors used for the control strategy. The J_{17} criterion assesses the computational resources required, which is represented by the dimension of the discrete state vector $\mathbf{x}_k^{\mathrm{c}}$, required for the control algorithm.

A summary of the evaluation criteria is presented in Table 1. The maximum uncontrolled responses required to calculate the evaluation criteria are given Tables 3-5, located in the Appendix A. All seventeen criteria should be reported for each proposed control strategy. The various levels of the respective earthquakes should each be considered in determining the evaluation criteria.

Researchers/designers are encouraged to include other criteria in their results if, through these criteria, important features of their control strategy can be demonstrated.

Table 1: Summary of Evaluation Criteria for the Nonlinear Benchmark Problem.

<table>
<tr>
<td>Interstory Drift Ratio
$J_1 = \max_{\substack{\text{El Centro}\\\text{Hachinohe}\\\text{Northridge}\\\text{Kobe}}} \left\{ \dfrac{\max\limits_{t,i} \dfrac{\lvert d_i(t)\rvert}{h_i}}{\delta^{\max}} \right\}$</td>
<td>Level Acceleration
$J_2 = \max_{\substack{\text{El Centro}\\\text{Hachinohe}\\\text{Northridge}\\\text{Kobe}}} \left\{ \dfrac{\max\limits_{t,i} \lvert \ddot{x}_{\mathrm{a}i}(t)\rvert}{\ddot{x}_{\mathrm{a}}^{\max}} \right\}$</td>
<td>Base Shear
$J_3 = \max_{\substack{\text{El Centro}\\\text{Hachinohe}\\\text{Northridge}\\\text{Kobe}}} \left\{ \dfrac{\max\limits_{t} \left\lvert \sum\limits_i m_i \ddot{x}_{\mathrm{a}i}(t)\right\rvert}{F_{\mathrm{b}}^{\max}} \right\}$</td>
</tr>
<tr>
<td>Normed Interstory Drift Ratio
$J_4 = \max_{\substack{\text{El Centro}\\\text{Hachinohe}\\\text{Northridge}\\\text{Kobe}}} \left\{ \dfrac{\max\limits_{i} \dfrac{\lVert d_i(t)\rVert}{h_i}}{\lVert \delta^{\max}\rVert} \right\}$</td>
<td>Normed Level Acceleration
$J_5 = \max_{\substack{\text{El Centro}\\\text{Hachinohe}\\\text{Northridge}\\\text{Kobe}}} \left\{ \dfrac{\max\limits_{i} \lVert \ddot{x}_{\mathrm{a}i}(t)\rVert}{\lVert \ddot{x}_{\mathrm{a}}^{\max}\rVert} \right\}$</td>
<td>Normed Base Shear
$J_6 = \max_{\substack{\text{El Centro}\\\text{Hachinohe}\\\text{Northridge}\\\text{Kobe}}} \left\{ \dfrac{\left\lVert \sum\limits_i m_i \ddot{x}_{\mathrm{a}i}(t)\right\rVert}{\lVert F_{\mathrm{b}}^{\max}\rVert} \right\}$</td>
</tr>
<tr>
<td>Ductility
$J_7 = \max_{\substack{\text{El Centro}\\\text{Hachinohe}\\\text{Northridge}\\\text{Kobe}}} \left\{ \dfrac{\max\limits_{t,j} \dfrac{\lvert \phi_j(t)\rvert}{\phi_{yj}}}{\phi^{\max}} \right\}$</td>
<td>Dissipated Energy
$J_8 = \max_{\substack{\text{El Centro}\\\text{Hachinohe}\\\text{Northridge}\\\text{Kobe}}} \left\{ \dfrac{\max\limits_{t,j} \dfrac{\int dE_j}{F_{yj}\cdot\phi_{yj}}}{E^{\max}} \right\}$</td>
<td>Plastic Connections
$J_9 = \max_{\substack{\text{El Centro}\\\text{Hachinohe}\\\text{Northridge}\\\text{Kobe}}} \left\{ \dfrac{N_{\mathrm{d}}^{\mathrm{C}}}{N_{\mathrm{d}}} \right\}$</td>
</tr>
<tr>
<td>Normed Ductility
$J_{10} = \max_{\substack{\text{El Centro}\\\text{Hachinohe}\\\text{Northridge}\\\text{Kobe}}} \left\{ \dfrac{\max\limits_{j} \dfrac{\lVert \phi_j(t)\rVert}{\phi_{yj}}}{\lVert \phi^{\max}\rVert} \right\}$</td>
<td>Control Force
$J_{11} = \max_{\substack{\text{El Centro}\\\text{Hachinohe}\\\text{Northridge}\\\text{Kobe}}} \left\{ \dfrac{\max\limits_{t,l} \lvert f_l(t)\rvert}{W} \right\}$</td>
<td>Control Device Stroke
$J_{12} = \max_{\substack{\text{El Centro}\\\text{Hachinohe}\\\text{Northridge}\\\text{Kobe}}} \left\{ \dfrac{\max\limits_{t,i} \lvert y_i^{\mathrm{a}}(t)\rvert}{x^{\max}} \right\}$</td>
</tr>
<tr>
<td>Control Power
$J_{13} = \max_{\substack{\text{El Centro}\\\text{Hachinohe}\\\text{Northridge}\\\text{Kobe}}} \left\{ \dfrac{\max\limits_{t} \left[\sum\limits_l \mathcal{P}_l(t)\right]}{\dot{x}^{\max} W} \right\}$</td>
<td>Normed Control Power
$J_{14} = \max_{\substack{\text{El Centro}\\\text{Hachinohe}\\\text{Northridge}\\\text{Kobe}}} \left\{ \dfrac{\sum\limits_l \dfrac{1}{t_f}\int_0^{t_f} \mathcal{P}_l(t)}{\dot{x}^{\max} W} \right\}$</td>
<td>Control Devices
J_{15} = Number of control devices
Sensors
J_{16} = Number of required sensors
Computational Resources
$J_{17} = \dim(\mathbf{x}_k^{\mathrm{c}})$</td>
</tr>
</table>

Control Implementation Constraints and Procedures

To make the benchmark problem as representative of the full-scale implementation as possible and to allow for direct comparison of the results submitted to the study, the following constraints and procedures are specified:

1. The measured outputs directly available for use in determination of the control action are the absolute horizontal acceleration and the interstory drift of each level of the structure. Although absolute velocity measurements are not available, they can be closely approximated by passing the measured accelerations through a second-order filter similar to that described in Spencer, *et al*. (1998a) but modified as appropriate for the bandwidth of the structures here.

2. The digitally implemented controller should have a sampling time between $0.001 \le T \le 0.01$ seconds.

3. The A/D and D/A converters on the digital controller have 16-bit precision and a span of ± 10 Volts.

4. Each of the measured responses contains an RMS noise of 0.03 Volts, which is approximately 0.3% of the full span of the A/D converters. The measurement noises are modeled as Gaussian rectangular pulse processes with a pulse width of 0.01 seconds.

5. No hard limit is placed on the number of states of the control algorithm, although the number of states should be kept to a reasonable number as limited computational resources in the digital controller exist. The designer/researcher should justify that the proposed algorithm(s) can be implemented with currently available computing hardware.

6. The control algorithm is required to be stable.

7. The performance of each control design should be evaluated for each of the earthquake records provided (*i.e*., El Centro, Hachinohe, Northridge and Kobe) and each of the levels specified for each earthquake. Performance should be evaluated assuming ideal actuators.

8. The closed loop stability robustness for each proposed active control design should be discussed.

9. If control device dynamics are included, the control signal to each control device has a constraint of 10 Volts for each respective earthquake; *i.e.*, $\max_{t,\,i} \left|u_i(t)\right| \le 10$ V.

10. The capabilities of each control device employed in the design should be discussed, and the designer/researcher should provide a justification of the availability of the device. Additional constraints unique to each control scheme should also be reported (*e.g*., maximum displacement, velocity, or force capacity of control devices). The control device model(s) should take the form of Eqs. (26)-(27) (i.e. actuator dynamics are neglected) when determining the evaluation criteria.

11. Researchers/designers should submit electronically a complete set of MATLAB files that will produce the evaluation criteria specified in this problem statement. For more details, see the *README* file included with the downloaded benchmark data on the benchmark homepage (*http://www.nd.edu/~quake/*).

Sample Control System Design

To illustrate some of the constraints and challenges of this benchmark problem, a sample control system is presented. Although the structure's response might be nonlinear during a severe earthquake, the sample control system is designed for the nominal linear structure. The sample control system design is included to serve as a guide to the participants in this study and is not intended to be a competitive design. The sample control system design will provide a structural control strategy for the 20-story benchmark building, including both N-S MRFs of this structure. The sample control system is a type of active system. The control actuators are located on each story of the structure to provide forces to the building. Feedback measurements are provided by accelerometers placed at various locations on the structure. In this section, the accelerometers chosen for the sample control system are described and models for the accelerometers are discussed. The control actuators are assumed to be ideal (*i.e.*, the dynamics of the actuators are neglected) for the sample control design. A linear quadratic Gaussian (LQG) control algorithm is designed based on a reduced order model of the system. Simulations are performed and evaluation criteria are determined and recorded here. The results of the sample control system design are discussed.

Sensors

Because accelerometers can readily provide reliable and inexpensive measurements of the absolute accelerations at arbitrary locations on a structure, the sample control system is based on acceleration feedback (Spencer, *et al.* 1994). A total of five acceleration measurements are selected for feedback in the control system: measurements on levels 4, 8, 12, 16 and 20.

A wide variety of accelerometers are available, many with a natural frequency at least an order of magnitude above the dynamics of this structure. Thus, each accelerometer is modeled as having a constant magnitude and phase. The magnitude of the output of each accelerometer is 10 V / *g* (where 1*g* = 9.81 m/sec^2), which is the sensitivity of the sensor. The measurement noise, prescribed in control implementation constraint 4, is included in the sensor model. Thus, in the form of Eqs. (22)-(23) the sensors can be modeled with $\mathbf{g}_5 = \mathbf{0}$ and

$$\mathbf{y}^s = \mathbf{D}_s \mathbf{y}_m + \mathbf{v} \tag{49}$$

where $\mathbf{D}_s = (10/9.81)[\mathbf{I}]$ V / (m/sec^2). Based on the measurements selected for feedback in the sample control strategy, $\mathbf{y}_m = [\ddot{x}_{a4} \ \ddot{x}_{a8} \ \ddot{x}_{a12} \ \ddot{x}_{a16} \ \ddot{x}_{a20}]^T$ in which the numeric subscript denotes the level.

For simulation purposes, the sensor block shown in Figure 11 is used to represent the five accelerometers used in the sample control system design.

Control Devices

Control actuators are placed throughout the above ground stories of the 20-story benchmark building, connecting adjacent levels. The size of the actuators are limited to provide maximum control forces of 1000 kN. Actuators with this capacity are readily available. To provide larger control forces at a particular location, multiple actuators can be employed. The control actuators for this sample control strategy are placed on each level of the structure, and a total of 25 actuators are used to control the 20-story benchmark building. Four actuators are located on the ground

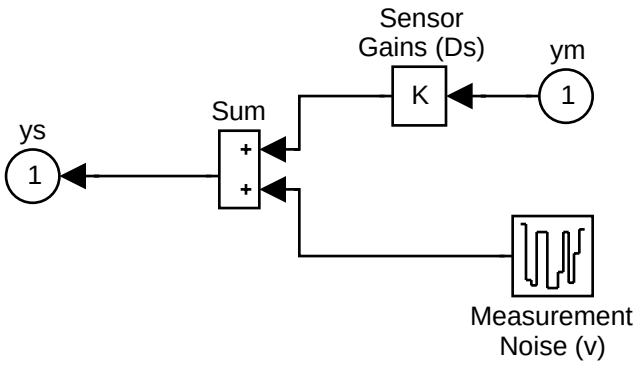

Figure 11. SIMULINK Block Representing the Sensors in the Sample Control System Design.

level, two actuators are located on each of the first and second levels, and one actuator is on each of the third through 19th levels of the structure. Each actuator is implemented in the structure using a chevron brace configuration, in which the actuator is horizontal and rigidly attached between the two consecutive levels of the building. Thus, the actuators placed on the first level will produce equal and opposite control forces on the first level and second level. In the analysis the compliance of the bracing is neglected. In the form of Eqs. (26) - (27), the force vector for the 25 control devices located on 20 levels of the building and producing 39 control forces (20 equal and opposite forces, less the force applied to the ground level) can be modeled as

$$\mathbf{f} = \mathbf{K}_f \mathbf{u} \tag{50}$$

$$\mathbf{y}_f = \begin{bmatrix} \mathbf{u} \\ \mathbf{y}_c \end{bmatrix} \tag{51}$$

where $\mathbf{K}_f$ is a matrix that accounts for multiple actuators per level and loads the control devices forces (per level) onto the building levels.

For simulation purposes, the control device block shown in Figure 12 is used to represent the ideal actuators used in the sample control system design. Note that the force gain, $\mathbf{K}_f$, in Figure 12 is the gain matrix from Eq. (50) that converts the control signal to control force, accounts for multiple actuators per level, and loads the actuator forces onto the 20 levels of the structure. This gain block represents the idealized actuator models.

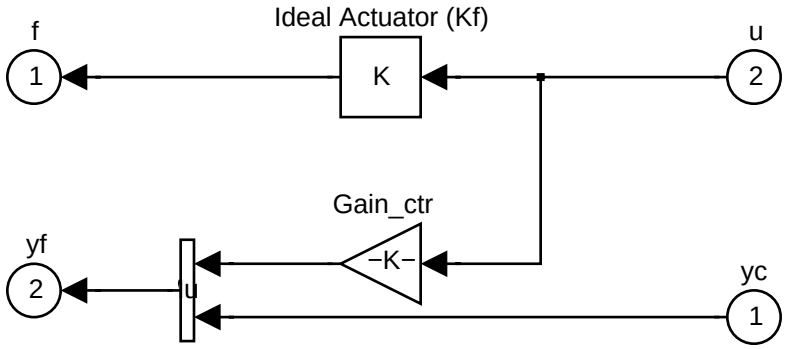

Figure 12. SIMULINK Block Representing the Control Devices in the Sample Control System Design.

Control Design Model

Because the evaluation model is quite large, a reduced order model of the system, designated the *design* model, is developed for purposes of control design. This 20-state reduced order design model of the 20-story structure is given as

$$\dot{\mathbf{x}}^{\mathrm{d}} = \mathbf{A}_{\mathrm{d}}\mathbf{x}^{\mathrm{d}} + \mathbf{B}_{\mathrm{d}}\mathbf{u} + \mathbf{E}_{\mathrm{d}}\ddot{x}_{\mathrm{g}} \tag{52}$$

$$\mathbf{y}_{\mathrm{sd}} = \mathbf{D}_{\mathrm{s}}(\mathbf{C}_{\mathrm{md}}\mathbf{x}^{\mathrm{d}} + \mathbf{D}_{\mathrm{md}}\mathbf{u} + \mathbf{F}_{\mathrm{md}}\ddot{x}_{\mathrm{g}}) + \mathbf{v} \tag{53}$$

$$\mathbf{y}_{\mathrm{ed}} = \mathbf{C}_{\mathrm{ed}}\mathbf{x}^{\mathrm{d}} + \mathbf{D}_{\mathrm{ed}}\mathbf{u} + \mathbf{F}_{\mathrm{ed}}\ddot{x}_{\mathrm{g}} \tag{54}$$

where $\mathbf{x}^{\mathrm{d}}$ is the design state vector, $\mathbf{y}_{\mathrm{md}} = [\ddot{x}_{\mathrm{a4}} \;\; \ddot{x}_{\mathrm{a8}} \;\; \ddot{x}_{\mathrm{a12}} \;\; \ddot{x}_{\mathrm{a16}} \;\; \ddot{x}_{\mathrm{a20}}]^{\mathrm{T}}$ is the vector of measured responses in Volts, $\mathbf{y}_{\mathrm{ed}} = [\ddot{x}_{\mathrm{a1}} \ldots \ddot{x}_{\mathrm{a20}}]^{\mathrm{T}}$ is the vector of regulated responses (lateral accelerations at each of the above ground levels), $\mathbf{u}$ is the control signal for the control force of the individual control devices neglecting actuator dynamics (note that of the 25 actuators, only 20 independent control forces are required, with the four actuators on the ground floor all exerting the same force, the two on the first level exerting the same force, and the two on the second level exerting the same force), and $\mathbf{A}_{\mathrm{d}}$, $\mathbf{B}_{\mathrm{d}}$, $\mathbf{E}_{\mathrm{d}}$, $\mathbf{C}_{\mathrm{md}}$, $\mathbf{C}_{\mathrm{ed}}$, $\mathbf{D}_{\mathrm{md}}$, $\mathbf{D}_{\mathrm{ed}}$, $\mathbf{F}_{\mathrm{md}}$ and $\mathbf{F}_{\mathrm{ed}}$ are the reduced order coefficient matrices. Notice that this design only makes use of the absolute accelerations of five levels of the structure for measured feedback, although additional measurements are available for feedback.

Control Algorithm

To illustrate some of the challenges of this benchmark problem, a sample linear quadratic Gaussian (LQG) control design is presented. To simplify design of the controller, $\ddot{x}_{\mathrm{g}}$ is taken to be a stationary white noise, and an infinite horizon performance index is chosen that weights the accelerations of the levels, *i.e.*,

$$\hat{J} = \lim_{\tau \to \infty} \frac{1}{\tau} \mathrm{E}\left[\int_0^{\tau} \left\{ (\mathbf{C}_{\mathrm{ed}}\mathbf{x}^{\mathrm{d}} + \mathbf{D}_{\mathrm{ed}}\mathbf{u})^{\mathrm{T}}\mathbf{Q}(\mathbf{C}_{\mathrm{ed}}\mathbf{x}^{\mathrm{d}} + \mathbf{D}_{\mathrm{ed}}\mathbf{u}) + \mathbf{R}\mathbf{u}^2 \right\} dt \right] \tag{55}$$

where $\mathbf{R}$ is a $[20 \times 20]$ matrix with equal weighting placed on each actuator force (*i.e.*, $\mathbf{R} = (1/16)[\mathbf{I}]$)and the weighting matrix $\mathbf{Q}$ was chosen to be a $[20 \times 20]$ matrix with equal weighting placed on each of the level accelerations (*i.e.*, $\mathbf{Q} = 3{\times}10^{9}[\mathbf{I}]$). Further, the measurement noises are assumed to be identically distributed, statistically independent Gaussian white noise processes, and $S_{\ddot{x}_g\ddot{x}_g}/S_{v_i v_i} = \gamma_g = 25$.

The separation principle allows the control and estimation problems to be considered separately, yielding a control law of the form (Stengel 1986; Skelton 1988)

$$\mathbf{u} = -\underset{\sim}{\mathbf{K}}\hat{\mathbf{x}}^{\mathrm{d}} \tag{56}$$

where $\hat{\mathbf{x}}^d$ is the Kalman Filter estimate of the state vector based on the reduced order design model, including the actuator models. By the certainty equivalence principle (Stengel 1986; Skelton 1988), $\underset{\sim}{\mathbf{K}}$ is the full state feedback gain matrix for the deterministic regulator problem given by

$$\underset{\sim}{\mathbf{K}} = \tilde{\mathbf{R}}^{-1}(\tilde{\mathbf{N}} + \mathbf{B}_d^T \underset{\sim}{\mathbf{P}}) \tag{57}$$

where $\underset{\sim}{\mathbf{P}}$ is the solution of the algebraic Riccati equation given by

$$\mathbf{0} = \underset{\sim}{\mathbf{P}}\tilde{\mathbf{A}} + \tilde{\mathbf{A}}^T \underset{\sim}{\mathbf{P}} - \underset{\sim}{\mathbf{P}}\mathbf{B}_d \tilde{\mathbf{R}}^{-1} \mathbf{B}_d^T \underset{\sim}{\mathbf{P}} + \tilde{\mathbf{Q}} \tag{58}$$

and

$$\tilde{\mathbf{Q}} = \mathbf{C}_{ed}^T \mathbf{Q} \mathbf{C}_{ed} - \tilde{\mathbf{N}} \tilde{\mathbf{R}}^{-1} \tilde{\mathbf{N}}^T \tag{59}$$

$$\tilde{\mathbf{N}} = \mathbf{C}_{ed}^T \mathbf{Q} \mathbf{D}_{ed} \tag{60}$$

$$\tilde{\mathbf{R}} = \mathbf{R} + \mathbf{D}_{ed}^T \mathbf{Q} \mathbf{D}_{ed} \tag{61}$$

$$\tilde{\mathbf{A}} = \mathbf{A}_d - \mathbf{B}_d \tilde{\mathbf{R}}^{-1} \tilde{\mathbf{N}}^T \tag{62}$$

Calculations to determine $\underset{\sim}{\mathbf{K}}$ were done using the MATLAB routine *lqry.m* within the control toolbox.

The Kalman Filter optimal estimator is given by

$$\dot{\hat{\mathbf{x}}}^d = \mathbf{A}_d \hat{\mathbf{x}}^d + \mathbf{B}_d \mathbf{u} + \mathbf{L}(\mathbf{y}_s - \mathbf{C}_{md} \hat{\mathbf{x}}^d - \mathbf{D}_{md} \mathbf{u}) \tag{63}$$

$$\mathbf{L} = [\underset{\sim}{\mathbf{R}}^{-1}(\gamma_g \mathbf{F}_{md} \mathbf{E}_d^T + \mathbf{C}_{md} \mathbf{S})]^T \tag{64}$$

where $\mathbf{S}$ is the solution of the algebraic Riccati equation given by

$$\mathbf{0} = \mathbf{S}\underset{\sim}{\mathbf{A}} + \underset{\sim}{\mathbf{A}}^T \mathbf{S} - \mathbf{S}\underset{\sim}{\mathbf{G}}\mathbf{S} + \underset{\sim}{\mathbf{H}} \tag{65}$$

and

$$\underset{\sim}{\mathbf{A}} = \mathbf{A}_d^T - \mathbf{C}_{md}^T \underset{\sim}{\mathbf{R}}^{-1}(\gamma_g \mathbf{F}_{md} \mathbf{E}_d^T) \tag{66}$$

$$\underset{\sim}{\mathbf{G}} = \mathbf{C}_{md}^T \underset{\sim}{\mathbf{R}}^{-1} \mathbf{C}_{md} \tag{67}$$

$$\underset{\sim}{\mathbf{H}} = \gamma_g \mathbf{E}_d \mathbf{E}_d^T - \gamma_g{}^2 \mathbf{E}_d \mathbf{F}_{md}^T \underset{\sim}{\mathbf{R}}^{-1} \mathbf{F}_{md} \mathbf{E}_d^T \tag{68}$$

$$\underset{\sim}{\mathbf{R}} = \mathbf{I} + \gamma_g \mathbf{F}_{md} \mathbf{F}_{md}^T \tag{69}$$

Calculations to determine $\mathbf{L}$ were done using the MATLAB routine *lqe.m* within the control toolbox.

Finally, the controller is put in the form of Eqs. (24)–(25) using the bilinear transformation (Antoniou, 1993) to yield the following compensator

$$\mathbf{x}_{k+1}^{c} = \underset{\sim}{\mathbf{A}}_{c}\mathbf{x}_{k}^{c} + \underset{\sim}{\mathbf{B}}_{c}\mathbf{y}_{k}^{s} \tag{70}$$

$$\mathbf{u}_{k} = \underset{\sim}{\mathbf{C}}_{c}\mathbf{x}_{k}^{c} + \underset{\sim}{\mathbf{D}}_{c}\mathbf{y}_{k}^{s}. \tag{71}$$

Calculations to determine the discrete time compensator were performed in MATLAB using the *c2dm.m* routine within the control toolbox. The control algorithm is implemented in simulation with the block illustrated in Figure 13. The A/D and D/A converter blocks are comprised of a saturation block in series with a quantizer, enforcing control implementation constraints 3 and 9.

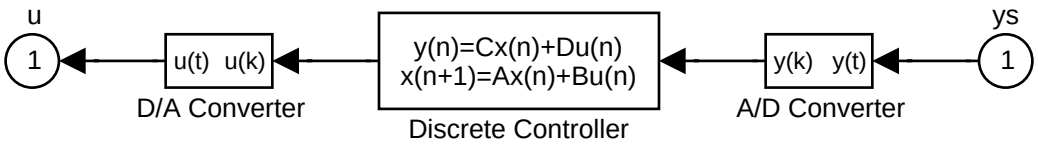

Figure 13. SIMULINK Block Representing the Control Algorithm in the Sample Control System Design.

Evaluation of Sample Control Design

The nonlinear 20-story benchmark model controlled with the linear sample control strategy described is evaluated. The sample control strategy is applied to the 20-story benchmark model. The responses of the controlled structure are determined for each of the 10 earthquake records using the MATLAB simulation discussed herein. Time histories of the acceleration response of the 20th level of the building for uncontrolled and controlled cases are shown in Figure 14 along with the maximum absolute acceleration and maximum drift ratio profiles over the height of each building. Only the original earthquake magnitudes are presented in this figure. It is clear from the time histories that the control strategy adds significant damping to the building system as well as provides moderate reduction of the maximum accelerations and drift ratios.

The structure's responses are used to calculate the performance indices (evaluation criteria) identified in this paper in order to discuss the performance. The performance of the sample control design is reported in Table 2. In this sample control strategy, the floor accelerations, both peak and normalized, are reduced substantially from the uncontrolled cases. The drift evaluation criteria are also reduced slightly, though the base shear criteria remain unaffected. The control force evaluation criteria are reasonable. The building damage evaluation criteria show overall improvement. The amount of energy dissipated through structural yielding is reduced substantially. The control device criteria appear reasonable. The number of sensors and control devices are also reasonable as well as the computational resources required to implement to 20-state controller. The sample control strategy provides adequate reduction of the evaluation criteria; however, let it be

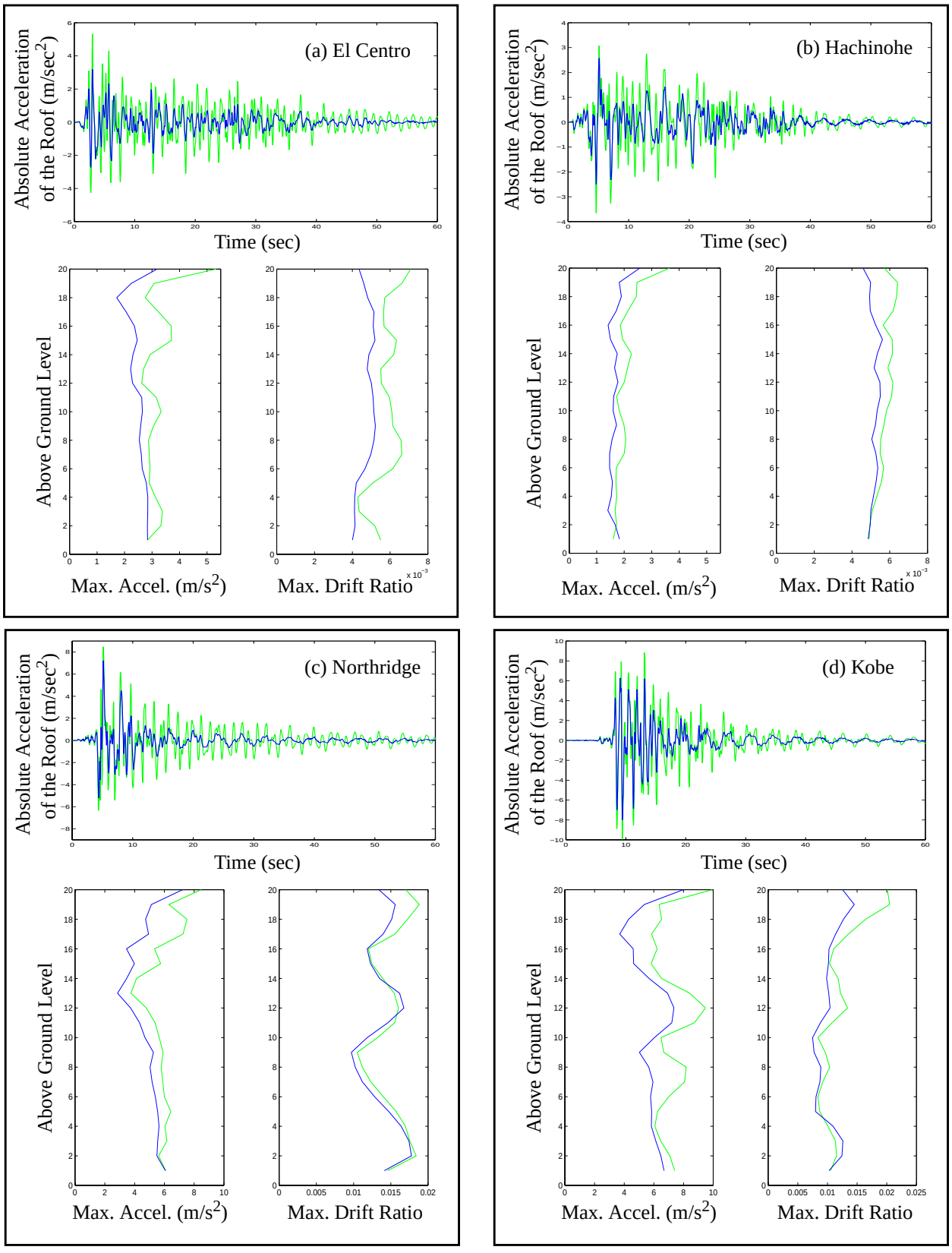

Figure 14. Uncontrolled (Dotted) and Controlled (Solid) Responses: (a) El Centro; (b) Hachinohe; (c) Northridge; and (d) Kobe.

Table 2: Earthquake Evaluation Criteria for the Sample Control Strategy.

Earthquake (intensity)	**El Centro (0.5/1.0/1.5)**	**Hachinohe (0.5/1.0/1.5)**	**Northridge (0.5/1.0)**	**Kobe (0.5/1.0)**	**Max Value**
J_1 Peak Drift Ratio	7.4732e-01 7.4831e-01 7.4762e-01	8.8310e-01 8.8697e-01 9.0656e-01	8.5857e-01 9.4211e-01	8.1611e-01 7.2778e-01	9.4211e-01
J_2 Peak Level Accel.	6.4758e-01 6.4609e-01 6.6412e-01	7.4578e-01 7.4292e-01 8.3269e-01	8.0678e-01 9.0432e-01	7.0209e-01 8.3914e-01	9.0432e-01
J_3 Peak Base Shear	7.8004e-01 7.8198e-01 9.0885e-01	9.7714e-01 9.8191e-01 1.0091e+00	8.8472e-01 9.6937e-01	9.2500e-01 1.0656e+00	1.0656e+00
J_4 Norm Drift Ratio	6.6243e-01 6.6287e-01 6.6964e-01	8.8464e-01 8.8399e-01 9.0272e-01	7.2391e-01 9.2948e-01	6.4772e-01 2.3033e-01	9.2948e-01
J_5 Norm Level Accel	5.6300e-01 5.5989e-01 5.7763e-01	6.5815e-01 6.5162e-01 6.6149e-01	5.9233e-01 6.3662e-01	5.7887e-01 7.1293e-01	7.1293e-01
J_6 Norm Base Shear	7.2441e-01 7.2328e-01 7.2916e-01	8.4922e-01 8.4788e-01 8.5766e-01	7.7585e-01 8.4075e-01	6.8868e-01 8.4043e-01	8.5766e-01
J_7 Ductility	7.7193e-01 7.7294e-01 7.2222e-01	9.5539e-01 9.5920e-01 9.4328e-01	7.2787e-01 9.7763e-01	6.8769e-01 6.8796e-01	9.7763e-01
J_8 Dissipated Energy	-- -- 7.8186e-02	-- -- 7.1441e-01	2.2047e-01 5.4786e-01	1.4443e-01 3.2294e-01	7.1441e-01
J_9 Plastic Connections	-- -- 3.7209e-01	-- -- 7.9070e-01	5.4167e-01 9.0625e-01	3.0769e-01 8.0952e-01	9.0625e-01
J_{10} Norm Ductility	7.3335e-01 7.3344e-01 6.5577e-01	8.4741e-01 8.4703e-01 8.8958e-01	6.3239e-01 9.4374e-01	7.7728e-01 2.2667e-01	9.4374e-01
J_{11} Control Force	1.6809e-03 3.3460e-03 5.0115e-03	1.9219e-03 3.5460e-03 5.0604e-03	6.7064e-03 8.1814e-03	4.9702e-03 8.9063e-03	8.9063e-03

Table 2: Earthquake Evaluation Criteria for the Sample Control Strategy.

Earthquake (intensity)	**El Centro (0.5/1.0/1.5)**	**Hachinohe (0.5/1.0/1.5)**	**Northridge (0.5/1.0)**	**Kobe (0.5/1.0)**	**Max Value**
J_{12} Device Stroke	7.2168e-02 7.2060e-02 7.2510e-02	7.5420e-02 7.5770e-02 8.0511e-02	7.8181e-02 1.0307e-01	1.2611e-01 1.1417e-01	1.2611e-01
J_{13} Control Power	1.2680e-03 2.4704e-03 3.8787e-03	8.2600e-04 1.6910e-03 2.5968e-03	4.0316e-03 5.1187e-03	4.0289e-03 8.8103e-03	8.8103e-03
J_{14} Norm Control Power	5.4943e-05 1.0279e-04 1.6110e-04	4.0700e-05 7.3444e-05 1.1333e-04	7.9195e-05 1.2176e-04	7.6991e-05 1.4546e-04	1.6110e-04
J_{15} Control Devices	25				25
J_{16} Sensors	5				5
J_{17} Comput'l Resources	20				20

stated again that this control strategy is intended to provide an example of the procedure for this benchmark problem and is not a competitive design.

Closure

The models and data for the nonlinear benchmark control problem for seismically excited buildings are available in a set of MATLAB files. Included are scripts which build the evaluation models of the 3-, 9- and 20-story buildings, perform the sample control design and run the simulation. These files are available on the World Wide Web at the following URL:

http://www.nd.edu/~quake/

If you cannot access the World Wide Web or have questions regarding the benchmark problem, please contact the senior author via e-mail at: spencer@nd.edu.

To increase the value of this effort to the community, participants in the nonlinear benchmark study are requested to submit their control designs electronically for inclusion on the benchmark homepage cited previously. This electronic submission should be in the form of an m-file script and the associated data that, when run, produces the evaluation criteria used defined in the problem statement. The file *Eval_NLBM.m* included with the sample control strategy is an example of the required evaluation m-file script. See the *README* file included with the downloaded benchmark data for more details.

Acknowledgements

The authors gratefully acknowledge the partial support of this research by the National Science Foundation under grants No. CMS 95-00301 and CMS 95-28083 (Dr. S. C. Liu, Program Director) and the Central Research Institute of Electric Power Industry in Japan. The authors would also like to acknowledge the generous efforts of Prof. Erik A. Johnson, University of Southern California Department of Civil and Environmental Engineering, in editing and providing detailed comments on this paper and the corresponding MATLAB programs.

References

Antoniou, A. (1993). *Digital Filters: Analysis, Design, and Applications*, McGraw-Hill, Inc., New York, pp.444–446.

Baker, G.A., Johnson, E.A. and Spencer, B.F., Jr. (1999). "Control Strategies for a Structural Control Benchmark Study: Verification by Experiment." *In the Proceedings of the 13th ASCE Engineering Mechanics Division Specialty Conference*, Johns Hopkins University, Baltimore, June13–16, 6 pages, (CD-ROM).

Balas, G.J. (1997). "Synthesis of Controllers for the Active Mass Driver System in the Presence of Uncertainty." *Proceedings of the ASCE Structures Congress XV*, 1997.

Bani-Hani, K., and Ghaboussi, J. (1998). "Nonlinear Structural Control Using Neural Networks.", *Journal of Engineering Mechanics*, Vol. 124, No. 3, pp.319–327.

Barrosa, L. R., (1999). "Performance evaluation of vibration controlled steel structures under seismic loading", Ph.D. thesis of Stanford University.

Caughey, T. K., (1998). "The Benchmark Problem." *Earthquake Engineering and Structural Dynamics*, Vol. 27, pp.1125.

Chang, K. C., Chen, S. J., and Lai, M. L. L., (1996). "Inelastic behavior of steel frames with added viscoelastic dampers." *Journal of Structural Engineering*, Vol 122, No. 10, pp.1178–1186.

Chen, J-C. Ed. (1996). *Proceedings of the 2nd International Workshop on Structural Control: Next Generation of Intelligent Structures*, Research Center, The Hong Kong University of Science and Technology (see *http://cwis.usc.edu/dept/civil_eng/structural/welcome.html*).

Clough, R.W. and Johnson, S. (1966). "Effect of stiffness degradation on earthquake ductility requirements." Proc. of the Japan Earthquake Engineering Symposium, Tokyo.

Cook, R.D., Malkus, D.S., Plesha, M.E. (1989). *Concepts and Applications of Finite Element Analysis*, John Wiley & Sons, New York.

Dyke, S.J., Spencer, B.F., Jr., Quast, P. and Sain, M.K. (1995). "The Role of Control-Structure Interaction in Protective System Design." *Journal of Engineering Mechanics, ASCE*, Vol.121, No. 2, pp.322–338.

Fujino, Y., Soong, T.T. and Spencer, B.F., Jr. (1996). "Structural Control: Basic Concepts and Applications." *Proceedings of the ASCE Structures Congress XIV*, Chicago, Illinois, pp. 1277–1287.

Giberson, M.F. (1967). "The response of nonlinear multistory structures subjected to earthquake excitation." Ph.D. Dissertation, Caltech.

Housner, G.W., et al., Masri, S.F., and Chassiakos, G.A., Eds. (1994). *Proceedings of the First World Conference on Structural Control*, International Association for Structural Control, Los Angels.

Housner, G.W., Bergman, L.A., Caughey, T.K., Chassiakos, A.G., Claus, R.O., Masri, S.F., Skelton, R.E., Soong, T.T., Spencer, B.F., Jr. and Yao, J.T.P. (1997). "Structural Control: Past, Present and Future," *Journal of Engineering Mechanics, ASCE*, Vol. 123, No. 9, pp. 897–971.

Lobo, R.F. (1994). “Inelastic Dynamic Analysis of Reinforced Concrete Structures in Three Dimensions.” *Ph.D. Dissertation*, Dept. of Civil Engrg. New York State University at Buffalo.

Lu, J., and Skelton, R.E. (1997). “Covariance Control Using Closed Loop Modeling for Structures.” *Proceedings of the ASCE Structures Congress XV*, 1997.

Masri, S.F., Bekey, G.A. and Caughey, T.K. (1981). “Optimum Pulse Control of Flexible Structures.” *Journal of Applied Mechanics*, Vol. 48, pp.619–626.

Masri, S.F., Bekey, G.A. and Caughey, T.K. (1982). “On-Line Control of Nonlinear Flexible Structures.” *Journal of Applied Mechanics*, Vol. 49, pp.877–884.

MATLAB (1997). The Math Works, Inc., Natick, Massachusetts.

Newmark, N.M. (1959) “A method of computation for structural dynamics” *Journal of Engineering Mechanics Division*, ASCE, Vol. 85, pp.67–94.

Ohtori, Y. and Spencer, B.F., Jr. (1999). “A MATLAB-Based Tool for Nonlinear Structural Analysis”, *In the Proceedings of the 13th ASCE Engineering Mechanics Division Specialty Conference*, Johns Hopkins University, Baltimore, June13–16, 6 pages, (CD-ROM).

Pantelides, C. P., and Nelson, P. A. (1995). “Continuous Pulse Control of Structures with material Nonlinearity.”, *Earthquake Engineering and Structural Dynamics*, Vol. 24, pp. 263–282.

Reinhorn, A.M., Manolis, G.D., and Wen, C.Y. (1987). “Active Control of Inelastic Structures.”, *Journal of Engineering Mechanics*, Vol. 113, No. 3, pp.315–333.

Sack, R.L., (1989). *Matrix Structural Analysis*, PWS-Kent Pub. Co., Boston.

Skelton, R.E. (1988). *Dynamic System Control: Linear Systems Analysis and Synthesis*. Wiley, New York.

Smith, H.A., Breneman, S.E. and Sureau, O. (1997). “H–infinity Static and Dynamic Output Feedback Control of the AMD Benchmark Problem.” *Proceedings of the ASCE Structures Congress XV*, 1997.

Soong, T.T. (1990). *Active Structural Control: Theory and Practice*, Longman Scientific and Technical, Essex, England.

Soong, T.T. and Constantinou, M.C., Eds. (1994). *Passive and Active Structural Vibration Control in Civil Engineering*, CISM Lecture Note, Springer-Verlag, New York.

Spencer, B.F., Jr., Suhardjo, J. and Sain, M.K. (1994). “Frequency Domain Optimal Control Strategies for Aseismic Protection.”, *Journal of Engineering Mechanics*, ASCE, Vol. 120, No.1, pp.135-159.

Spencer, B.F., Jr., Dyke, S.J., and Deoskar, H.S. (1997). “Benchmark Problem in Structural Control.”, *Proceeding of the ASCE Structural Congress XV*, Vol. 2, pp.1265-1269.

Spencer, B.F., Jr., Dyke, S.J. and Deoskar, H.S. (1998a,b). “Benchmark Problems in Structural Control – Part I: Active Mass Driver System; Part II: Active Tendon System.” *Earthquake Engneering. and Structural Dynamics*, Vol. 27, No. 11, pp.1127–2247.

Spencer, B.F., Jr. and Sain, M.K. (1997) “Controlling Buildings: A New Frontier in Feedback,” *IEEE Control Systems Magazine: Special Issue on Emerging Technologies* (Tariq Samad Guest Ed.), Vol. 17, No. 6, pp. 19–35.

Spencer, B.F., Jr., Christenson, R.E. and Dyke, S.J. (1999). “Next Generation Benchmark Control Problems for Seismically Excited Buildings.” *Proc., 2nd World Conf. on Structural Control*, (T. Kobori, et al., eds., Wiley), Vol.2, pp.1135–1360.

Stengel, R.F. (1986). *Stochastic Optimal Control: Theory and Application*. Wiley, New York.

Subbaraj, K. and Dokainish, M.A. (1989). “A Survey of Direct Time-Integration Methods in Computational Structural Dynamics - II. Implicit Method.” *Computers and Structures.*, Vol.32, No. 6, pp.1387–1401.

Tsai, C. S., Chen, K. C., and Chen, C. S. (1998). “Nonlinear Behavior of Structures with Added Passive Devices.”, *Proceedings of Second World Conference on Structural Control*, Kyoto, Japan, Vol. 1, pp.309–318.

Valles, R.E., Reinhorn, A.M., Kunnath, S.K., Li, C. and Madan, A. (1996). “IDARC2D Version4.0: A Computer Program for the Inelastic Damage Analysis of the Buildings.” *Technical Report NCEER-96-0010, Nat. Ctr. for Earthquake Engrg. Res.,* Buffalo, New York.

Wu, J.C., Agrawal, A.K. and Yang J.N. (1997). “Application of Sliding Mode Control to a Benchmark Problem.” *Proceedings of the ASCE Structures Congress XV,* 1997.

Yang, J. N., Li, Z., and Liu, S.C. (1992). “Control of Hysteretic System Using Velocity and Acceleration Feedbacks.” *Journal of Engineering Mechanics,* Vol.118, No. 11, pp.2227–2245.

Yang, J. N., Li, Z., and Vongchavalitkul, S. (1994). “Generalization of Optimal Control Theory: Linear and Nonlinear Control.”, *Journal of Engineering Mechanics,* Vol. 120, No. 2, pp.266–283.

Yang, J. N., Wu, J. C., and Agrawal, A. K. (1995). “Sliding Mode Control for Nonlinear and Hysteretic Structures.”, *Journal of Engineering Mechanics,* Vol. 121, No. 12, pp.1330–1339.

Yang, J. N., Wu, J. C., Samali, B., and Agrawal, A. K. (1999). “A Benchmark Problem for Response Control of Wind-Excited Tall Buildings.” *Proc., 2nd World Conf. on Structural Control,* (T. Kobori, et al., eds., Wiley), Vol.2, pp.1408–1416.

Appendix A: Uncontrolled Responses

Table 3: Uncontrolled Response Quantities for the 3-Story Benchmark Building (integration time step = 0.005 sec)

Earthquake (intensity)	El Centro (0.5/1.0/1.5)	Hachinohe (0.5/1.0/1.5)	Northridge (0.5/1.0)	Kobe (0.5/1.0)
δ^{max}	1.0529e-02 1.5034e-02 1.7136e-02	8.7308e-03 1.4491e-02 2.0449e-02	1.8433e-02 2.5292e-02	1.9929e-02 3.6526e-02
$\ddot{x}_a^{max}$ (m/sec^2)	4.2820e+00 6.5389e+00 7.4044e+00	3.9299e+00 6.4800e+00 6.9300e+00	7.2971e+00 9.5898e+00	7.3332e+00 1.2035e+01
F_b^{max} (N)	8.9267e+06 1.0120e+07 1.0978e+07	6.8201e+06 9.6532e+06 1.1374e+07	1.2542e+07 1.4225e+07	1.1148e+07 1.3369e+07
$\lVert\delta^{max}\rVert$	1.3148e-03 2.4586e-03 4.2633e-03	1.7714e-03 3.1946e-03 4.4445e-03	7.3560e-03 9.1753e-03	4.5279e-03 1.0031e-02
$\lVert\ddot{x}_a^{max}\rVert$ (m/sec^2)	5.6856e-01 9.2382e-01 1.2678e+00	7.3930e-01 1.2113e+00 1.4789e+00	7.1020e-01 1.0539e+00	8.7806e-01 1.1339e+00
$\lVert F_b^{max}\rVert$ (N)	1.0311e+06 1.6609e+06 2.2803e+06	1.3891e+06 2.2709e+06 2.7837e+06	1.2341e+06 1.9531e+06	1.5471e+06 1.9071e+06
ϕ^{max}	1.1186e+00 1.8119e+00 2.2866e+00	8.6224e-01 1.7610e+00 2.2747e+00	3.0339e+00 4.1131e+00	2.3134e+00 3.9848e+00
E^{max}	1.8401e+00 9.1945e+01 1.8260e+02	-- 1.0729e+02 2.7485e+02	3.7655e+01 1.8877e+02	1.0430e+02 2.5011e+02
N_d	2.0000e+00 2.2000e+01 2.2000e+01	-- 2.2000e+01 2.4000e+01	2.4000e+01 3.3000e+01	2.4000e+01 3.2000e+01
$\lVert\phi^{max}\rVert$	1.3509e-01 3.8657e-01 6.7595e-01	1.7583e-01 3.7202e-01 6.0460e-01	1.3877e+00 1.4097e+00	5.7743e-01 1.3249e+00
x^{max} (m)	1.0491e-01 1.5073e-01 1.7202e-01	9.0144e-02 1.4653e-01 1.8510e-01	1.6690e-01 2.7151e-01	1.9294e-01 3.0690e-01
$\dot{x}^{max}$ (m/sec)	7.8298e-01 9.5484e-01 1.2267e+00	5.3705e-01 8.8999e-01 9.2899e-01	1.1126e+00 1.4105e+00	1.3988e+00 1.8750e+00

Table 4: Uncontrolled Response Quantities for the 9-Story Benchmark Building (integration time step = 0.005 sec)

Earthquake (intensity)	El Centro (0.5/1.0/1.5)	Hachinohe (0.5/1.0/1.5)	Northridge (0.5/1.0)	Kobe (0.5/1.0)
δ^{max}	8.5680e-03 1.5088e-02 2.1311e-02	6.9973e-03 1.3336e-02 1.9413e-02	1.5453e-02 2.0871e-02	2.1616e-02 2.9315e-02
$\ddot{x}_a^{max}$ (m/sec^2)	3.2884e+00 5.4153e+00 6.1457e+00	2.5913e+00 5.1598e+00 6.0303e+00	5.6327e+00 7.3395e+00	6.9249e+00 1.0097e+01
F_b^{max} (N)	1.1581e+07 1.7337e+07 1.9400e+07	9.9777e+06 1.6710e+07 1.8261e+07	1.7985e+07 2.1233e+07	1.4707e+07 2.0813e+07
$\lVert\delta^{max}\rVert$	1.5064e-03 2.4850e-03 3.6308e-03	1.1758e-03 2.2736e-03 4.1847e-03	3.1206e-03 3.7980e-03	3.7216e-03 6.6937e-03
$\lVert\ddot{x}_a^{max}\rVert$ (m/sec^2)	5.7698e-01 9.7837e-01 1.2604e+00	3.7648e-01 6.9060e-01 9.0154e-01	8.2840e-01 9.3598e-01	7.0597e-01 8.9825e-01
$\lVert F_b^{max}\rVert$ (N)	1.8315e+06 2.8483e+06 3.3887e+06	1.6650e+06 3.1243e+06 4.2257e+06	4.1269e+06 4.4983e+06	1.7684e+06 2.2577e+06
ϕ^{max}	8.7286e-01 2.1145e+00 3.1185e+00	7.5391e-01 1.8784e+00 2.0809e+00	2.1660e+00 2.8399e+00	2.4609e+00 3.1837e+00
E^{max}	-- 1.5704e+01 4.0527e+01	-- 1.6693e+01 4.3983e+01	3.2348e+01 8.9588e+01	7.4119e+01 2.4428e+02
N_d	-- 4.9000e+01 6.9000e+01	-- 5.7000e+01 7.1000e+01	6.3000e+01 7.5000e+01	2.6000e+01 7.6000e+01
$\lVert\phi^{max}\rVert$	1.4043e-01 3.0245e-01 6.2741e-01	1.2737e-01 3.0150e-01 6.7259e-01	3.7622e-01 5.2675e-01	4.5631e-01 1.3378e+00
x^{max} (m)	2.0010e-01 3.8509e-01 4.8825e-01	1.8627e-01 3.7228e-01 4.6111e-01	4.4937e-01 6.1972e-01	3.0704e-01 4.7760e-01
$\dot{x}^{max}$ (m/sec)	8.3503e-01 1.3814e+00 1.4688e+00	6.5607e-01 1.1492e+00 1.1501e+00	1.6355e+00 2.3196e+00	1.1205e+00 1.9751e+00

Table 5: Uncontrolled Response Quantities for the 20-Story Benchmark Building (integration time step = 0.01 sec)

Earthquake (intensity)	El Centro (0.5/1.0/1.5)	Hachinohe (0.5/1.0/1.5)	Northridge (0.5/1.0)	Kobe (0.5/1.0)
δ^{max}	3.5418e-03 7.0835e-03 1.0640e-02	3.2055e-03 6.4111e-03 9.1585e-03	1.0899e-02 1.8820e-02	1.0807e-02 2.0481e-02
$\ddot{x}_a^{max}$ (m/sec^2)	2.6696e+00 5.3392e+00 7.7856e+00	1.8291e+00 3.6582e+00 4.7152e+00	6.0076e+00 8.5107e+00	7.4945e+00 9.9741e+00
F_b^{max} (N)	3.6882e+06 7.3765e+06 9.5282e+06	3.1784e+06 6.3568e+06 9.1234e+06	1.0363e+07 1.4257e+07	1.0079e+07 1.1423e+07
$\lVert\delta^{max}\rVert$	6.7334e-04 1.3467e-03 2.0001e-03	6.0306e-04 1.2061e-03 1.7664e-03	1.8994e-03 6.6722e-03	1.4874e-03 7.3706e-03
$\lVert\ddot{x}_a^{max}\rVert$ (m/sec^2)	3.8851e-01 7.7702e-01 1.1286e+00	2.7580e-01 5.5161e-01 8.0448e-01	8.0270e-01 1.0136e+00	7.5885e-01 1.0029e+00
$\lVert F_b^{max}\rVert$ (N)	7.6393e+05 1.5279e+06 2.2728e+06	7.0643e+05 1.4129e+06 2.0821e+06	2.1527e+06 2.3912e+06	1.6258e+06 2.0298e+06
ϕ^{max}	4.6630e-01 9.3259e-01 1.5032e+00	4.2780e-01 8.5560e-01 1.3970e+00	1.6753e+00 3.3601e+00	1.9229e+00 3.1987e+00
E^{max}	-- -- 1.9465e+01	-- -- 6.0923e+00	2.0605e+01 8.6226e+01	1.8701e+01 2.8269e+02
N_d	-- -- 8.6000e+01	-- -- 8.6000e+01	9.6000e+01 1.9200e+02	7.8000e+01 1.6800e+02
$\lVert\phi^{max}\rVert$	9.8637e-02 1.9727e-01 3.3098e-01	9.3745e-02 1.8749e-01 2.7843e-01	3.6294e-01 1.4056e+00	2.4164e-01 1.4228e+00
x^{max} (m)	1.5219e-01 3.0439e-01 4.5352e-01	1.7397e-01 3.4795e-01 4.9178e-01	4.8940e-01 7.5036e-01	3.1409e-01 5.1734e-01
$\dot{x}^{max}$ (m/sec)	4.5783e-01 9.1566e-01 1.3007e+00	4.5122e-01 9.0244e-01 1.2684e+00	1.6616e+00 2.0390e+00	1.3145e+00 1.8458e+00

Appendix B: Nomenclature

Nomenclature

$\tilde{\mathbf{A}}$ – matrix used in the solution of the algebraic Riccati equation

$\underset{\sim}{\mathbf{A}}$ – matrix used in the solution of the algebraic Riccati equation

$\mathbf{A}_d$, $\mathbf{B}_d$, $\mathbf{E}_d$ – state space matrices for the reduced order design model

α_{AA}, α_{BB} – concentrated plasticity parameters

β – Parameter for Newmark-β method

$\mathbf{C}$ – Global damping matrix

$\hat{\mathbf{C}}$ – Damping matrix for reduced system

$\mathbf{C}_{md}$, $\mathbf{D}_{md}$, $\mathbf{F}_{md}$ – state space matrices for the reduced order evaluation model used to specify the measured responses

$\mathbf{C}_{ed}$, $\mathbf{D}_{ed}$, $\mathbf{F}_{ed}$ – state space matrices for the reduced order evaluation model used to specify the regulated responses

c_1, c_2 – parameters for Rayleigh damping

$\mathbf{D}_s$ – sensor gain

d_i – interstory drift of above ground levels (m)

$\Delta\mathbf{F}_{err}$ – vector of the unbalanced force (N)

$\Delta\mathbf{F}_D$ – equivalent force of the incremental equation of motion (N)

$\Delta\mathbf{f}$ – incremental control force (N)

Δt – time interval for Newmark-β integration (sec)

$\Delta\mathbf{U}$ – incremental response vector

$\Delta\mathbf{U}_{act}$ – incremental response vector for active degrees of freedom

$\Delta\mathbf{U}_{slv}$ – incremental response vector for slave degrees of freedom

$\Delta\ddot{x}_g$ – ground acceleration increment (m/sec^2)

δ^{max} – maximum interstory drift ratio for each respective earthquake

$\|\delta^{max}\|$ – the maximum normed interstory drift ratio corresponding to the uncontrolled structure excited by each respective earthquake

$E[\cdot]$ – expected value operator used in the infinite horizon performance index for the sample LQG

E^{max} – maximum dissipated energy of the uncontrolled structure

EI_A, EI_B, EI_O – flexural stiffness at end A, end B, and center of member, respectively.

ζ_i – damping in the *i*-th mode of the evaluation model

F_b^{max} – maximum base shear (N)

$\left\|F_b^{max}\right\|$ – the maximum normed uncontrolled base shear for each respective earthquake (N)

F_{yj} – yield moment at the end of the *j*-th member

$\mathbf{f}$ – vector of forces produced by the control device(s) (kN)

$f_{AA}, f_{AB}, f_{BA}, f_{BB}$ $f_{AA'}, f_{AB'}, f_{BB'}$ – flexibility coefficients

f_l – control force of the *l*-th control device (N)

$\mathbf{G}$ – loading vector of ground acceleration to the structure

$\tilde{\mathbf{G}}$ – matrix used in the solution of the algebraic Riccati equation

$\mathbf{GA}$ – shear stiffness of member

g – gravitational constant (9.81 m/sec^2)

$\mathbf{g}_1(\cdot) \rightarrow \mathbf{g}_4(\cdot)$ – functions defining the evaluation model

$\mathbf{g}_5(\cdot), \mathbf{g}_6(\cdot)$ – sensor dynamics for the sensor(s)

$\mathbf{g}_7(\cdot), \mathbf{g}_8(\cdot)$ – functions defining the feedback controller

$\mathbf{g}_9(\cdot) \rightarrow \mathbf{g}_{11}(\cdot)$ – functions defining the control device(s)

γ – parameter for Newmark-β method

γ_g – ratio of autospectral densities for Gaussian white noise

$\tilde{\mathbf{H}}$ – matrix used in the solution of the algebraic Riccati equation

h_i – height of the *i*-th level (m)

$\mathbf{I}$ – identity matrix

J_i – *i*-th evaluation criteria

$\hat{J}$ – infinite horizon performance index

$\mathbf{K}$ – global stiffness matrix of structure

$\mathbf{K}_t$ – tangent stiffness matrix of structure at time t

$\mathbf{K}_D$ – equivalent dynamic stiffness matrix

$\mathbf{K}_f$ – matrix to account for multiple actuators and to load control forces onto building

$\hat{\mathbf{K}}$ – global stiffness matrix for reduced system

$\tilde{\mathbf{K}}$ – full state feedback gain matrix for the deterministic regulator problem

k – discrete time step index

k_{AA} , k_{AB} , k_{BA} , k_{BB} – stiffness matrix coefficient

L – length of member (m)

$\mathbf{L}$ – Kalman Filter optimal estimator

l – index of control devices

$\mathbf{M}$ – global mass matrix

$\hat{\mathbf{M}}$ – global mass matrix for reduced system

m_i – seismic mass (including framing) of the *i*-th level

$\tilde{\mathbf{N}}$ – matrix used in the solution of the algebraic Riccati equation

$\mathbf{N}_d$ – number of damaged connections of the uncontrolled structure

$\mathbf{N}_d^C$ – number of damaged connections of the structure with the applied control strategy

n – index of global DOFs

$\mathbf{P}$ – vector defining the loading of control forces onto the structure

$\underset{\sim}{\mathbf{P}}$ – solution of the algebraic Riccati equation

p – index of local DOFs

$\hat{\mathbf{\Phi}}$ – mode vector for reduced system

$\mathcal{P}_i$ – measure of the instantaneous power required by the active control actuators

$\|\mathcal{P}_i\|$ – measure of the total power required by the *i*th actuator for the entire seismic event

ϕ_j – curvature at the ends of the *j*-th member

ϕ_{yj} – yield curvature at the ends of the *j*-th member

ϕ^{max} – maximum curvature of the uncontrolled structure

$\|\phi^{max}\|$ – normed maximum curvature at the member ends

$\mathbf{Q}$ – weighting matrix of responses for LQG control design

$\tilde{\mathbf{Q}}$ – matrix used in the solution of the algebraic Riccati equation

q – index for node number

$\mathbf{R}$ – weighting matrix of control forces for LQG control design

$\tilde{\mathbf{R}}$ – matrix used in the solution of the algebraic Riccati equation

$\underset{\sim}{\mathbf{R}}$ – matrix used in the solution of the algebraic Riccati equation

$\mathbf{S}$ – solution of the algebraic Riccati equation

$S_{v_i v_i}$ – autospectral density function of measurement noise

$S_{\ddot{x}_g \ddot{x}_g}$ – autospectral density function of ground acceleration

T – sampling time (sec)

$\mathbf{T}_{\mathrm{R}}$ – transformation matrix for rigid floor

t – continuous time step index (sec)

t_{f} – sufficiently large time to allow the response of the structure to attenuate (sec)

$\mathbf{U}_t$ – response vector at time t

$\mathbf{u}$ – continuous vector control output (sample and hold of $\mathbf{u}_k$) (Volts)

$\mathbf{u}_k$ – vector control output at time $t = kT$ for the feedback compensator (Volts)

$\mathbf{v}$ – measurement noise vector for the sensors

W – seismic weight of the structure (N)

ω_i – natural (undamped) frequency of the i-th mode of the evaluation model

$\mathbf{x}$ – state vector for the evaluation model

$\mathbf{x}^{\mathrm{a}}$ – continuous time state vector for the control device

x_i – i-th state of evaluation model

$\mathbf{x}_k^{\mathrm{c}}$ – state vector for the discrete feedback compensator at time $t = kT$

$x^{\max}$ – maximum uncontrolled displacement relative to ground for each respective earthquake (m)

$\left\| x^{\max} \right\|$ – the maximum normed uncontrolled displacement of the levels for each respective earthquake (m)

$\mathbf{x}^{\mathrm{d}}$ – continuous state vector for the design model

$\hat{\mathbf{x}}^{\mathrm{d}}$ – Kalman Filter estimate of the state vector for the design model

$\mathbf{x}^{\mathrm{s}}$ – state vector of the sensor model

$\dot{x}^{\max}$ – maximum uncontrolled velocity relative to ground (m/sec)

$\ddot{x}_{\mathrm{a}i}$ – absolute acceleration of the ith level (m/sec^2)

$\ddot{x}_{\mathrm{a}}^{\max}$ – maximum uncontrolled absolute roof acceleration (m/sec^2)

$\left\| \ddot{x}_{\mathrm{a}}^{\max} \right\|$ – the maximum normed absolute acceleration of the uncontrolled structure excited by each respective earthquake $(\mathrm{m} \cdot \mathrm{sec}^{-3/2})$

$\ddot{x}_{\mathrm{g}}$ – absolute acceleration of the ground (m/sec^2)

y_l^{a} – displacement of the l-th control device (m)

$\dot{y}_l^{\mathrm{a}}$ – velocity of the l-th control device (m/sec)

$\mathbf{y}_{\mathrm{c}}$ – vector of connector responses of evaluation model

$\mathbf{y}_{\mathrm{cd}}$ – vector of connection responses of reduced order design model

$\mathbf{y}_{\mathrm{e}}$ – vector of evaluation responses of evaluation model

$\mathbf{y}_{\mathrm{f}}$ – vector of control device responses

$\mathbf{y}_{\mathrm{m}}$ – vector of measured responses of evaluation model

$\mathbf{y}_{\mathrm{md}}$ – vector of measured responses of design model

$\mathbf{y}^{\mathrm{s}}$ – vector of responses of sensor model

$\mathbf{y}_{k}^{\mathrm{s}}$ – discrete vector of responses of sensor model

$\mathbf{y}_{\mathrm{ed}}$ – vector of regulated responses of design model

$|\cdot|$ – absolute value operator

$||\cdot||$ – normed operator

$\int dE_j$ – dissipated energy at the ends of the j-th member.